

49

1449

NACA CASE FILE COPY

RESEARCH MEMORANDUM

THE LONGITUDINAL CHARACTERISTICS AT MACH NUMBERS
UP TO 0.9 OF A WING-FUSELAGE-TAIL COMBINATION
HAVING A WING WITH 40° OF SWEEPBACK AND
AN ASPECT RATIO OF 10

By Bruce E. Tinling

Ames Aeronautical Laboratory
Moffett Field, Calif.

CLASSIFICATION CHANGED TO UNCLASSIFIED

AUTHORITY: J.W.CROWLEY DATE: 9-15-55

CHANGE NO. 3095

WHL

~~CLASSIFIED DOCUMENT~~

This material contains information affecting the National Defense of the United States within the meaning of the espionage laws, Title 18, U.S.C., Secs. 793 and 794, the transmission or revelation of which in any manner to an unauthorized person is prohibited by law.

**NATIONAL ADVISORY COMMITTEE
FOR AERONAUTICS**

WASHINGTON

December 12, 1952

NACA RM A52I19

0371234.034

DECLASSIFIED

CONFIDENTIAL

1S

NACA RM A52119

NATIONAL ADVISORY COMMITTEE FOR AERONAUTICS

RESEARCH MEMORANDUM

THE LONGITUDINAL CHARACTERISTICS AT MACH NUMBERS
UP TO 0.9 OF A WING-FUSELAGE-TAIL COMBINATION
HAVING A WING WITH 40° OF SWEEPBACK AND
AN ASPECT RATIO OF 10

By Bruce E. Tinling

SUMMARY

An investigation has been conducted to evaluate the effects of an all-movable horizontal tail on the longitudinal characteristics of a swept-back wing and a fuselage of a type suitable for long-range high-speed airplanes. The wing, which was cambered and twisted, had an aspect ratio of 10, a taper ratio of 0.4, and 40° of sweepback. The all-movable horizontal tail had an aspect ratio of 4.5, a taper ratio of 0.4, and 40° of sweepback. Wind-tunnel tests were conducted at Reynolds numbers of 2,000,000 and 8,000,000 at low speed and at Mach numbers from 0.25 to 0.90 at a Reynolds number of 2,000,000.

It was found that a large reduction of the longitudinal stability of the wing-fuselage-tail combination occurred at lift coefficients well below the stall. Analysis of the low-speed results indicated that this reduction of longitudinal stability was caused primarily by decreases in the longitudinal stability of the wing-fuselage combination. The use of four fences resulted in nearly constant longitudinal stability of the wing-fuselage-tail combination up to the stall at low speeds, and for lift coefficients up to about 0.7 at Mach numbers from 0.6 to 0.9. The all-movable horizontal tail provided nearly constant control effectiveness throughout the lift range at each Mach number.

CONFIDENTIAL

INTRODUCTION

The aerodynamic problems associated with a configuration considered suitable for long-range airplanes to fly at high subsonic speeds have been the subject of an investigation in the Ames 12-foot pressure wind tunnel. The longitudinal characteristics of a high-aspect-ratio swept wing in combination with a fuselage of high fineness ratio have been presented in reference 1. The present paper is concerned primarily with the effects of an all-movable horizontal tail on the longitudinal characteristics of this wing-fuselage combination.

The results of reference 1 indicate that the pitching-moment characteristics of the wing, which had 40° of sweepback and an aspect ratio of 10, were considerably improved by the use of fences. The initial tests during the present phase of the investigation were therefore directed toward determining whether fences are necessary for the attainment of satisfactory tail-on pitching-moment characteristics. A limited number of tests were also conducted to determine the effects of tail height. A series of tests with four fences on the wing was conducted for several tail incidences to evaluate the longitudinal characteristics of this configuration and the control effectiveness of the all-movable horizontal tail. These tests were conducted at Mach numbers of 0.165 and 0.25 at a Reynolds number of 8,000,000 and at Mach numbers from 0.25 to 0.90 at a Reynolds number of 2,000,000. The lift and pitching-moment of the isolated horizontal tail were also measured over this Mach number and Reynolds number range.

NOTATION

Symbols and Parameters

- a mean line designation, fraction of chord over which design load is uniform
- $\frac{b}{2}$ wing semispan perpendicular to the plane of symmetry
- C_D drag coefficient $\left(\frac{\text{drag}}{qS} \right)$
- C_L lift coefficient $\left(\frac{\text{lift}}{qS} \right)$

- C_m pitching-moment coefficient about the quarter point of the mean aerodynamic chord $\left(\frac{\text{pitching moment}}{qS\bar{c}} \right)$
 (See fig. 1(a) for location of wing moment center with respect to the fuselage.)
- c local chord parallel to the plane of symmetry
- c' local chord normal to the reference sweep line
- c_{av} average chord $\left(\frac{2S}{b} \right)$
- \bar{c} mean aerodynamic chord $\left(\frac{\int_0^{b/2} c^2 dy}{\int_0^{b/2} c dy} \right)$
- c_l section lift coefficient
- c_{l_i} design section lift coefficient
- i_t incidence of the horizontal tail with respect to the wing root chord
- l_t tail length, distance between the quarter points of the mean aerodynamic chords of the wing and the horizontal tail
- M free-stream Mach number
- q free-stream dynamic pressure
- R Reynolds number, based on the wing mean aerodynamic chord
- S area of semispan wing or horizontal tail
- t section maximum thickness
- y lateral distance from the plane of symmetry
- α angle of attack of the wing chord at the plane of symmetry (referred to herein as the wing root chord)
- ϵ effective average downwash angle
- ϕ angle of twist, positive for washin, measured in planes parallel to the plane of symmetry

$$\Delta C_m = K_1 C_{L_w} \quad (\text{Tail off})$$

$$\Delta C_m = K_1 C_{L_w} - \left[(\Delta \epsilon - \Delta \alpha) \frac{\partial C_m}{\partial i_t} \right] \quad (\text{Tail on})$$

where

$$\Delta \epsilon = K_2 C_{L_w}$$

The values of $\partial C_m / \partial i_t$ were obtained from the test results. The values of K_1 and K_2 for each Mach number calculated by the method of reference 3 are given in the following table:

| M | K_1 | K_2 |
|-------|--------|-------|
| 0.165 | 0.0030 | 0.71 |
| .25 | .0032 | .72 |
| .60 | .0048 | .77 |
| .80 | .0069 | .81 |
| .86 | .0078 | .83 |
| .90 | .0087 | .85 |

Since the turntable upon which the model was mounted was directly connected to the balance system, a tare correction to the drag was necessary. This correction was determined by multiplying the drag force on the turntable, as determined from tests with the model removed from the wind tunnel, by the fraction of the turntable not covered by the model fuselage. The following corrections were subtracted from the measured drag coefficients:

| M | R | $C_{D_{tare}}$ |
|-------|-----------|----------------|
| 0.165 | 8,000,000 | 0.0025 |
| .25 | 8,000,000 | .0024 |
| .25 | 2,000,000 | .0025 |
| .60 | 2,000,000 | .0025 |
| .80 | 2,000,000 | .0028 |
| .86 | 2,000,000 | .0030 |
| .90 | 2,000,000 | .0032 |

No attempt has been made to evaluate tares due to interference between the model and the turntable or to compensate for the tunnel-floor boundary layer which, at the turntable, had a displacement thickness of one-half inch.

RESULTS AND DISCUSSION

Effect of Wing Fences

The data of reference 1 have shown that the pitching-moment characteristics of the wing-fuselage combination can be improved through the use of fences. As would be expected, the fences caused a similar improvement in the pitching-moment characteristics of the wing-fuselage-tail combination. (See fig. 3.) These data show that large reductions of static longitudinal stability at lift coefficients less than that for the stall were avoided through the use of four fences on the wing.

The pitching-moment contribution of the horizontal tail was not changed significantly by the addition of the wing fences, as may be seen from figure 4. This indicates that the addition of wing fences caused little or no change in either the average effective downwash angle or the tail efficiency factor. The improvement of the tail-on pitching-moment characteristics caused by fences, therefore, was primarily due to improvements of the longitudinal characteristics of the wing-fuselage combination.

Effect of Tail Height

The effect of increasing the tail height $0.05 b/2$ is shown in figure 5. These data are for the three-fence configuration. (See fig. 1(c).) The change in tail height had no significant effect on the large changes in stability which occurred in the upper lift-coefficient range at the higher Mach numbers. At lower lift coefficients, the longitudinal stability and lift coefficient for balance were somewhat greater for the higher tail position. Both these effects may have been caused by an improvement in the tail efficiency factor $\eta(q_t/q)$ resulting from moving the tail from the fuselage center line to a position above the fuselage.

Longitudinal Characteristics of the Model
With Four Wing Fences

The effectiveness of the horizontal tail, both as a stabilizer and as a longitudinal control when mounted in the plane of the wing root chord and leading edge, was evaluated from data obtained with four fences on the wing. (See fig. 1(c).) The aerodynamic characteristics

of this configuration at a Reynolds number of 8,000,000 and a Mach number of 0.165 (125 miles per hour at sea level) for a tail incidence of -4° are presented in figure 6. The longitudinal stability under these conditions is indicated to be constant up to a lift coefficient of about 1.5 ($\alpha = 20^\circ$). It was not possible to attain maximum lift at this Mach number due to the angle-of-attack limitation with the fuselage installed. The stall is believed to have been imminent, however, since the results from reference 1 show that the wing alone stalled at an angle of attack of 21° .

Lift, drag, and pitching-moment data for several tail incidences are shown in figure 7. At a Mach number of 0.25 and a Reynolds number of 8,000,000 (fig. 7(a)), the variation of pitching moment with lift was nearly linear and the control effectiveness $\partial C_m / \partial i_t$ was about -0.030 at lift coefficients up to the stall. It can be noted from figure 7(a) that the pitching-moment curves are more nearly linear with the tail on than with the tail off, the tail-off stability decreasing with increasing lift. The comparatively constant tail-on stability results from an increase with increasing lift coefficient of the stability contribution of the horizontal tail. This contribution, if the increment in the lift-curve slope due to the horizontal tail is neglected, is proportional to

$$\frac{(dC_L/d\alpha)_t}{(dC_L/d\alpha)_{w+f}} \left[\eta \left(\frac{q_t}{q} \right) \right] \left(1 - \frac{d\epsilon}{d\alpha} \right)$$

Calculations to evaluate the average effective downwash angle and the tail efficiency factor were made using the force data of figure 7 and the isolated tail data of figure 8. These calculations were performed in the same manner as in reference 4. In choosing the lift-curve slope of the isolated horizontal tail used in calculating $\eta(q_t/q)$, it was assumed that the Mach number at the tail was the same as the free-stream Mach number. The results of the calculations for a Mach number of 0.25 and a Reynolds number of 8,000,000 indicate nearly constant values of the tail efficiency factor $\eta(q_t/q)$ and of the rate of change of effective downwash with angle of attack $d\epsilon/d\alpha$ up to a lift coefficient of 1.0. (See fig. 9.) The factor

$$\frac{(dC_L/d\alpha)_t}{(dC_L/d\alpha)_{w+f}}$$

however, increases at the higher lift coefficients in a manner which compensates for the reduction of the stability of the wing-fuselage combination. This compensating effect is not mere coincidence, since,

on a swept wing, a reduction of lift-curve slope usually occurs simultaneously with a reduction of longitudinal stability.

The data for Mach numbers from 0.60 to 0.90 (figs. 7(c) to 7(f)) indicate nearly constant longitudinal stability and control effectiveness up to a lift coefficient of about 0.7 at each Mach number. At approximately this lift coefficient, the longitudinal stability decreased for a small range of lift coefficients and then increased with further increase in lift coefficient. This increase in tail-on stability is opposite that which occurs with the tail off. The data of figure 10 show that this effect is due primarily to a large increase in the ratio

$$\frac{(dC_L/d\alpha)_t}{(dC_L/d\alpha)_{w+f}}$$

As in the low-speed case, the increase was caused by a reduction in wing lift-curve slope which accompanied a reduction in the stability of the wing-fuselage combination.

The effect of Mach number on the tail control-effectiveness parameter $\partial C_m / \partial i_t$ and the tail-on pitching-moment-curve slope dC_m / dC_L at a lift coefficient of 0.4 is presented in figure 11. From these data it may be seen that the control effectiveness increased about 17 percent between Mach numbers of 0.25 and 0.90. Within the same Mach number range, the pitching-moment-curve slope varied about 0.06. The variation with Mach number of the factors contributing to the control effectiveness and to the tail-on pitching-moment-curve slope has also been included in figure 11.

Estimation of Average Effective Downwash

The effective downwash angles in the plane of the wing root chord and leading edge evaluated from the test results are presented as a function of angle of attack in figure 12. The theoretical variation of downwash with angle of attack in this plane and the position of the center of the wake were calculated by the method of reference 5. The variation of loading, as well as the variation of downwash angle, across the span of the horizontal tail was taken into account when calculating the average effective downwash. The results of these calculations are presented in figures 13 and 14. In applying the method of reference 5, it was found that the calculated downwash was sensitive to small changes in the wing loading, especially near the plane of symmetry. The theoretical loading and lift-curve slope were calculated by the modified Falkner 19X1 method which, as indicated in reference 6, yields accurate

results for swept-back wings of high aspect ratio. Account was taken of the effect of the fuselage on the loading according to the method outlined in reference 7. It was also necessary to account for the effects of wing incidence with respect to the fuselage. This was accomplished by assuming an altered twist distribution near the root section such that the chord at the plane of symmetry had an angle of attack equal to that of the fuselage center line. The results of these calculations are compared with unpublished experimental loadings for Mach numbers of 0.25 and 0.80 in figure 15. Both the theoretical and the experimental loadings were used in obtaining the theoretical downwash by the method of reference 5. The accuracy of this method in predicting downwash for this wing may be ascertained from the following table:

| M | $d\epsilon/d\alpha$, measured at $\alpha=0$ | | |
|------|--|--------------------------------------|---------------------------------------|
| | Experiment | Theoretical - Theoretical loading | Theoretical - Experimental loading |
| 0.25 | 0.18 | 0.30 | 0.26 |
| .80 | .28 | .37 | .37 |

From these data it may be seen that the theoretical method overestimates the average effective downwash by a considerable amount. As a consequence, the stability contribution of the horizontal tail, which is dependent upon $1 - d\epsilon/d\alpha$, would be underestimated by as much as 15 percent if the theoretical values of $d\epsilon/d\alpha$ were used. As noted previously, the theoretical values of downwash were found to be sensitive to small changes in wing loading, especially near the plane of symmetry. For example, the theoretical loading at 15 percent of the semispan at a Mach number of 0.25 differed from the experimental loading by only 4 percent, yet the values of downwash calculated for the two loadings differed by about 14 percent.

CONCLUDING REMARKS

The results of wind-tunnel tests to evaluate the longitudinal characteristics of a wing-fuselage-tail combination suitable for a long-range airplane to fly at high subsonic speeds have been presented. The wing had 40° of sweepback and an aspect ratio of 10. The all-movable horizontal tail had 40° of sweepback and an aspect ratio of 4.5.

The results of this investigation indicate that at a low Mach number, corresponding to a speed of 125 miles per hour at sea level, the static longitudinal stability of the wing-fuselage-tail combination with four

DECLASSIFIED

wing fences was nearly constant up to a lift coefficient of 1.5. For a given Mach number in the range from 0.6 to 0.9, the static longitudinal stability was nearly constant for lift coefficients up to about 0.7. At a lift coefficient of 0.4, the variation of pitching-moment-curve slope between Mach numbers of 0.25 and 0.90 was about 0.06. The all-movable horizontal tail provided nearly constant control effectiveness throughout the lift range for a given Mach number, and its effectiveness increased by about 17 percent in the Mach number range from 0.25 to 0.90.

Without fences, there were large reductions in the longitudinal stability of the wing-fuselage-tail combination in the high-lift range. These reductions were caused primarily by changes in the static longitudinal stability of the wing-fuselage combination.

Ames Aeronautical Laboratory
National Advisory Committee for Aeronautics
Moffett Field, Calif.

REFERENCES

1. Edwards, George G., Tinling, Bruce E., and Ackerman, Arthur C.: The Longitudinal Characteristics at Mach Numbers up to 0.92 of a Cambered and Twisted Wing Having 40° of Sweepback and an Aspect Ratio of 10. NACA RM A52F18, 1952.
2. Herriot, John G.: Blockage Corrections for Three-Dimensional-Flow Closed-Throat Wind Tunnels With Consideration of the Effect of Compressibility. NACA Rep. 995, 1950. (Formerly NACA RM A7B28)
3. Sivells, James C., and Salmi, Rachel M.: Jet-Boundary Corrections for Complete and Semispan Swept Wings in Closed Circular Wind Tunnels. NACA TN 2454, 1951.
4. Johnson, Ben H., Jr., and Rollins, Francis W.: Investigation of a Thin Wing of Aspect Ratio 4 in the Ames 12-foot Pressure Wind Tunnel. V - Static Longitudinal Stability and Control Throughout the Subsonic Speed Range of a Semispan Model of a Supersonic Airplane. NACA RM A9I01, 1949.
5. Diederich, Franklin W.: Charts and Tables for Use in Calculations of Downwash of Wings of Arbitrary Plan Form. NACA TN 2353, 1951.
6. Schneider, William C.: A Comparison of the Spanwise Loading Calculated by Various Methods With Experimental Loadings Obtained on a 45° Swept-Back Wing of Aspect Ratio 8 at a Reynolds Number of 4.0×10^6 . NACA RM L51G30, 1952.

CONFIDENTIAL

0371201030

7. Martina, Albert P.: The Interference Effects of a Body on the Spanwise Load Distributions of Two 45° Swept-Back Wings of Aspect Ratio 8 From Low-Speed Tests at a Reynolds Number of 4×10^6 . NACA RM L51K23, 1952.

TABLE I.— GEOMETRICAL PROPERTIES OF THE MODEL

| | |
|---|--|
| Wing (Reference sweep line: Locus of quarter chords of sections inclined 40° to plane of symmetry) | |
| Aspect ratio | 10.0 |
| Taper ratio | 0.4 |
| Sweepback | 40° |
| Twist (washout at tip) | 5° |
| Reference sections (normal to reference sweep line) | |
| Root | NACA 0014, $a=0.8$ (modified) $c_{l_i} = 0.4$ |
| Tip | NACA 0011, $a=0.8$ (modified) $c_{l_i} = 0.4$ |
| Area (semispan model) | 6.944 ft ² |
| Mean aerodynamic chord | 1.251 ft |
| Horizontal tail (Reference sweep line: Locus of quarter chords of sections inclined 40° to plane of symmetry) | |
| Aspect ratio | 4.5 |
| Taper ratio | 0.4 |
| Sweepback | 40° |
| Reference sections | NACA 0010 |
| Tail length, l_t | $3.25\bar{c}$ |
| Area (semispan model) | 1.387 ft ² |
| Mean aerodynamic chord | 0.833 ft |
| Tail volume, l_t/\bar{c} (S_t/S_w) | 0.65 |
| Tail heights (measured from the intersection of the fuselage center line and the plane of the wing root chord and leading edge) | |
| | .0 or 0.05 $b/2$ |

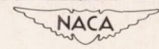


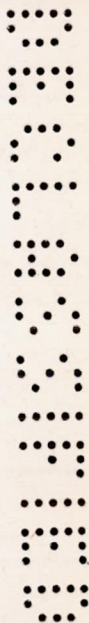
TABLE I.- CONCLUDED

Fuselage

Fineness ratio 12.6
 Fuselage coordinates:

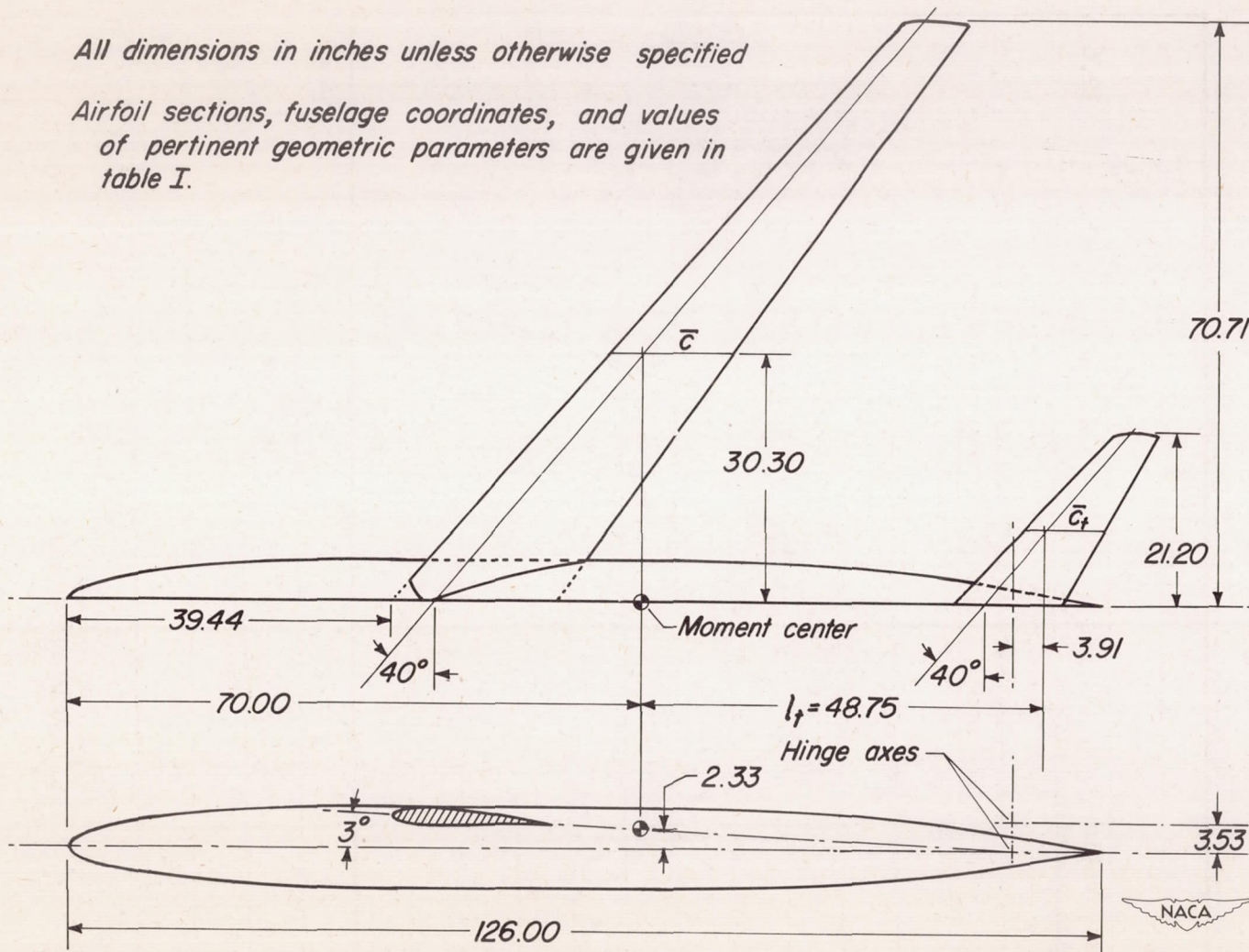
| <u>Distance from nose, inches</u> | <u>Radius, inches</u> |
|---------------------------------------|---------------------------|
| 0 | 0 |
| 1.27 | 1.04 |
| 2.54 | 1.57 |
| 5.08 | 2.35 |
| 10.16 | 3.36 |
| 20.31 | 4.44 |
| 30.47 | 4.90 |
| 39.44 | 5.00 |
| 50.00 | 5.00 |
| 60.00 | 5.00 |
| 70.00 | 5.00 |
| 76.00 | 4.96 |
| 82.00 | 4.83 |
| 88.00 | 4.61 |
| 94.00 | 4.27 |
| 100.00 | 3.77 |
| 106.00 | 3.03 |
| 126.00 | 0 |





All dimensions in inches unless otherwise specified

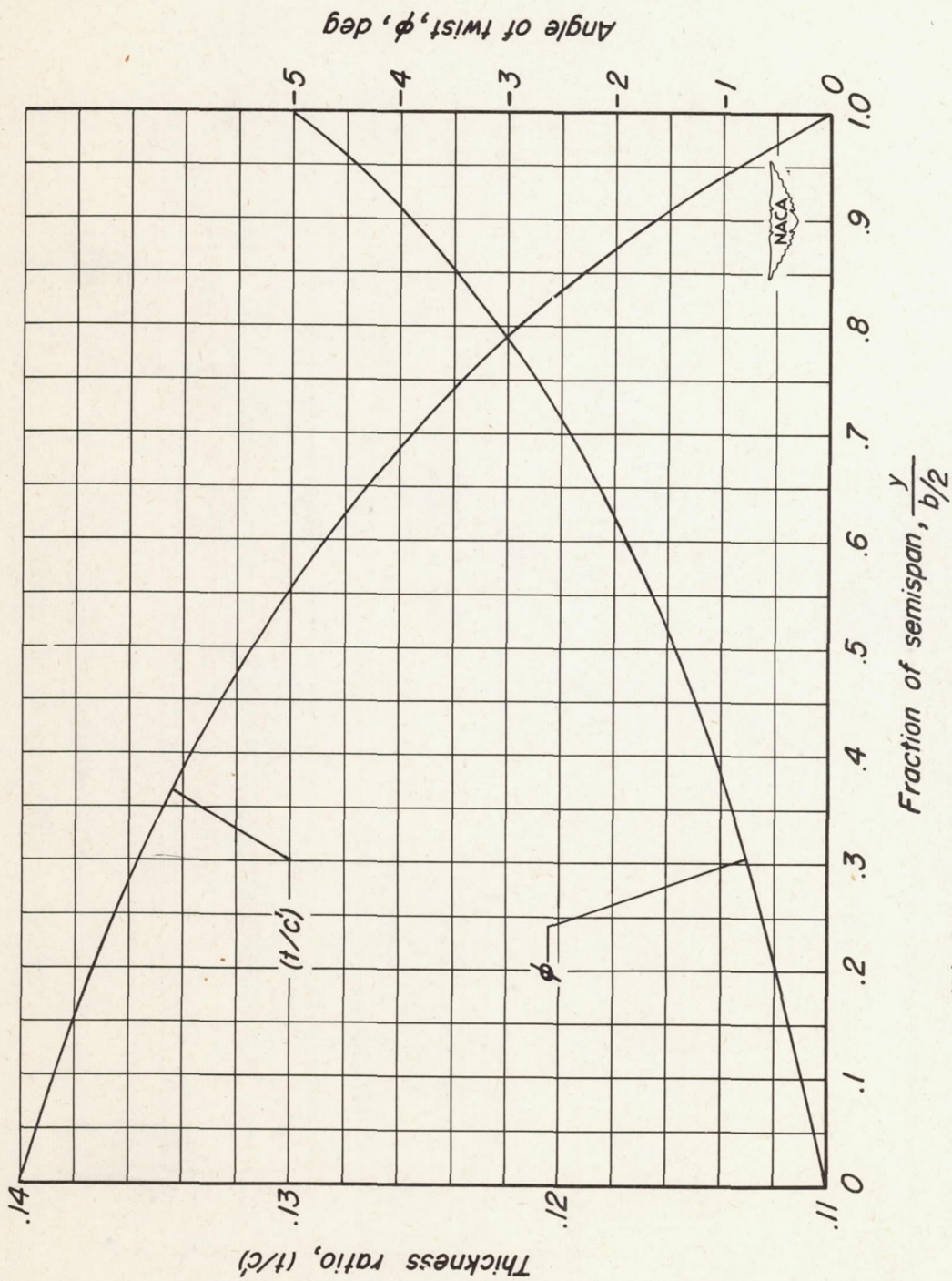
Airfoil sections, fuselage coordinates, and values of pertinent geometric parameters are given in table I.



(a) Dimensions.

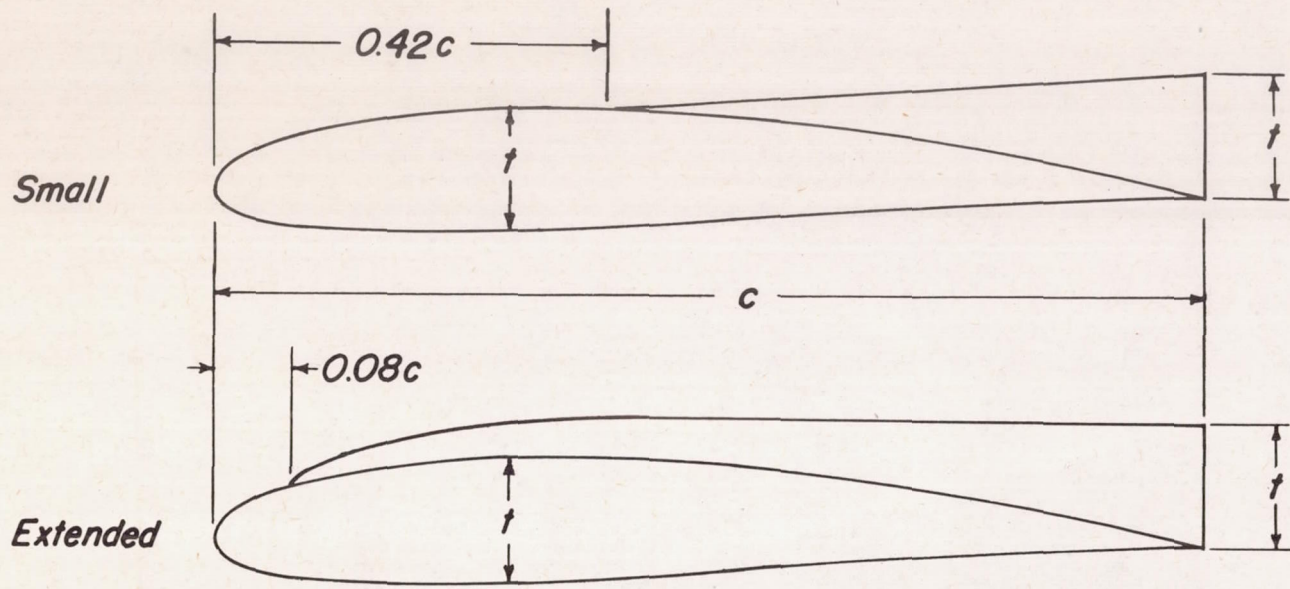
Figure 1.- Geometry of the model.

CONFIDENTIAL



(b) Distribution of twist and thickness ratio.

Figure 1. - Continued.



CONFIDENTIAL

| Configuration | Type and location |
|---------------|--|
| Three fences | Small at $\frac{y}{b/2} = 0.33, 0.50, \text{ and } 0.75$ |
| Four fences | Small at $\frac{y}{b/2} = 0.33$ Extended at $\frac{y}{b/2} = 0.50, 0.70, \text{ and } 0.85$ |

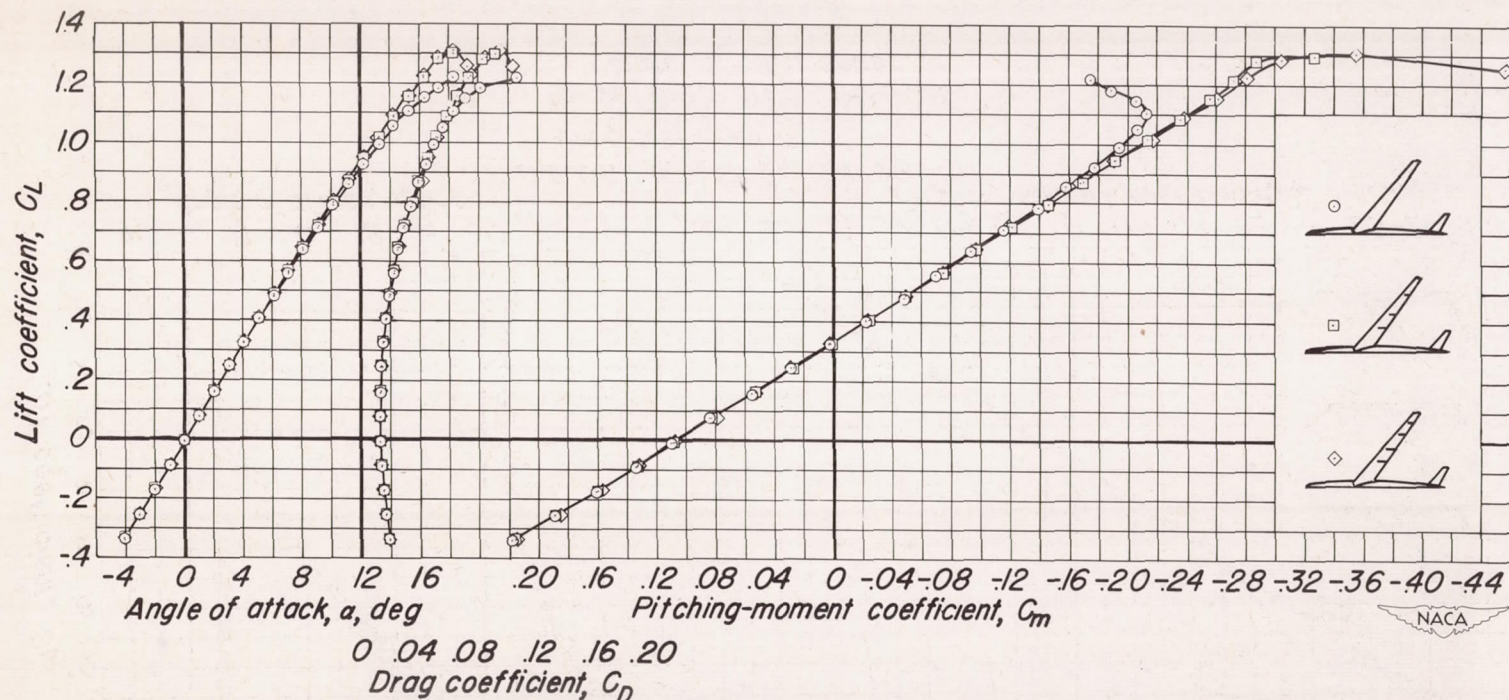


(c) Fence details.
Figure 1.- Concluded.

0371201030



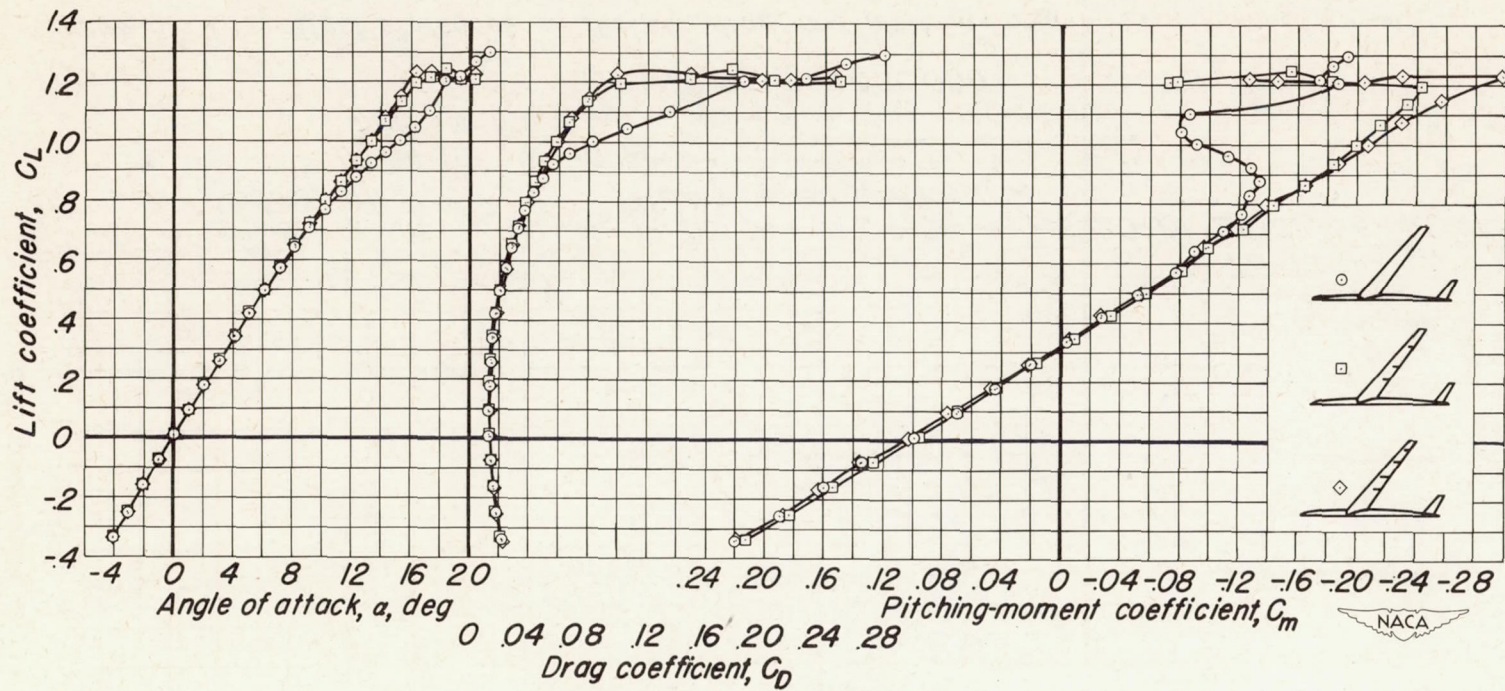
Figure 2.- Photograph of the model mounted in the wind tunnel.



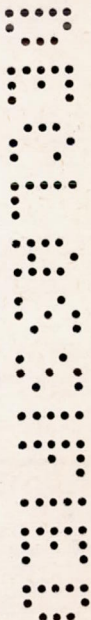
0 .04 .08 .12 .16 .20
 Drag coefficient, C_D

(a) $M=0.25, R=8,000,000$.

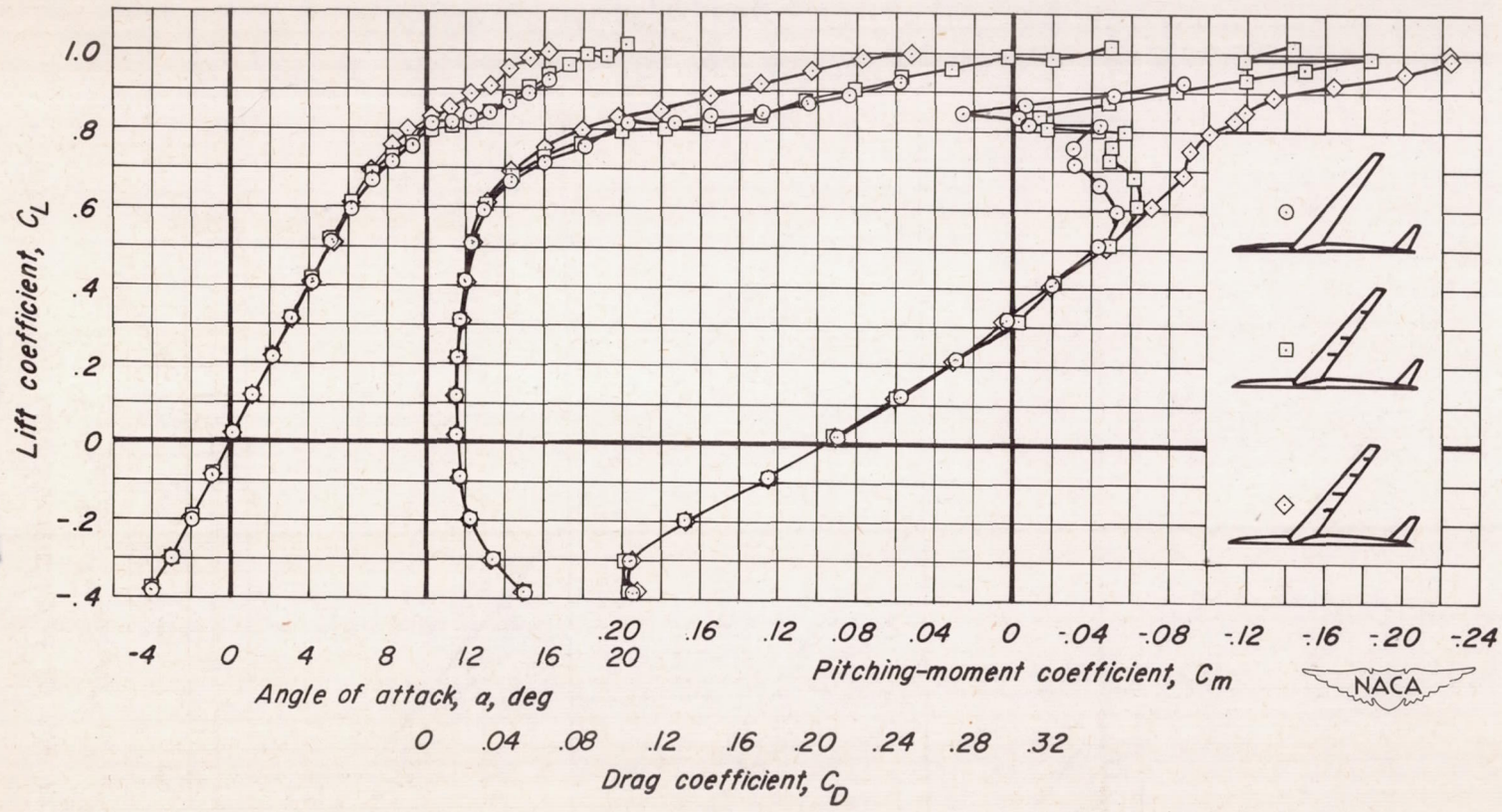
Figure 3.- The effect of fences on the lift, drag, and pitching-moment coefficients. $i_1 = -4^\circ$.



(b) $M=0.25$, $R=2,000,000$.
Figure 3.- Continued.



CONFIDENTIAL



(c) $M=0.80, R=2,000,000.$

Figure 3.-Concluded.

CONFIDENTIAL

Pitching - moment coefficient due to the horizontal tail,
($C_{m_{tail}}$ on $\bar{C}_{m_{tail}}$ off)

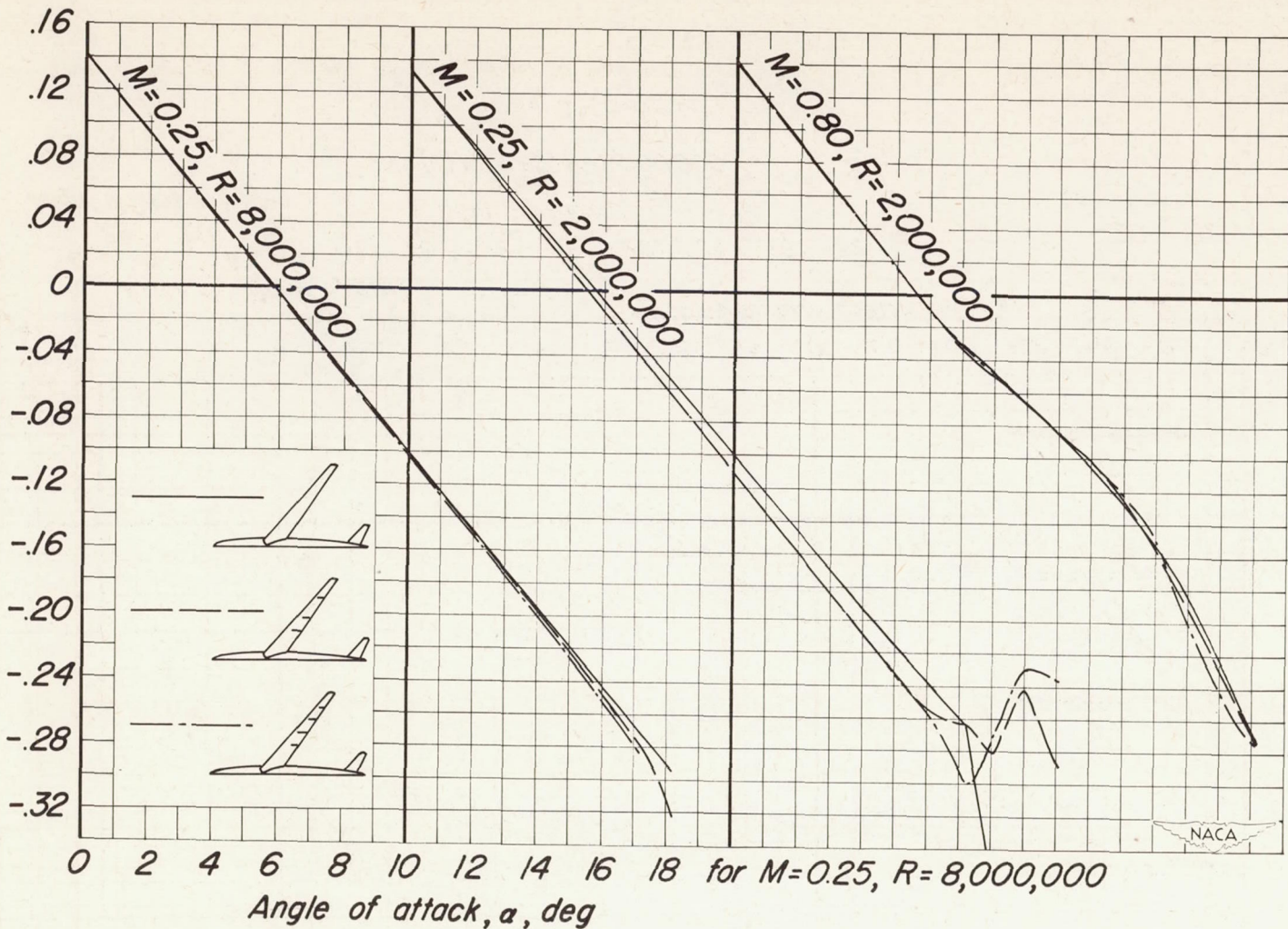
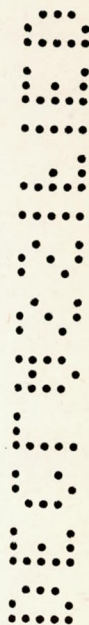
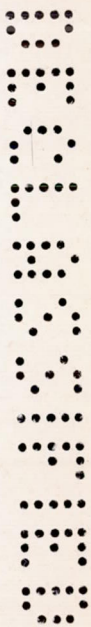
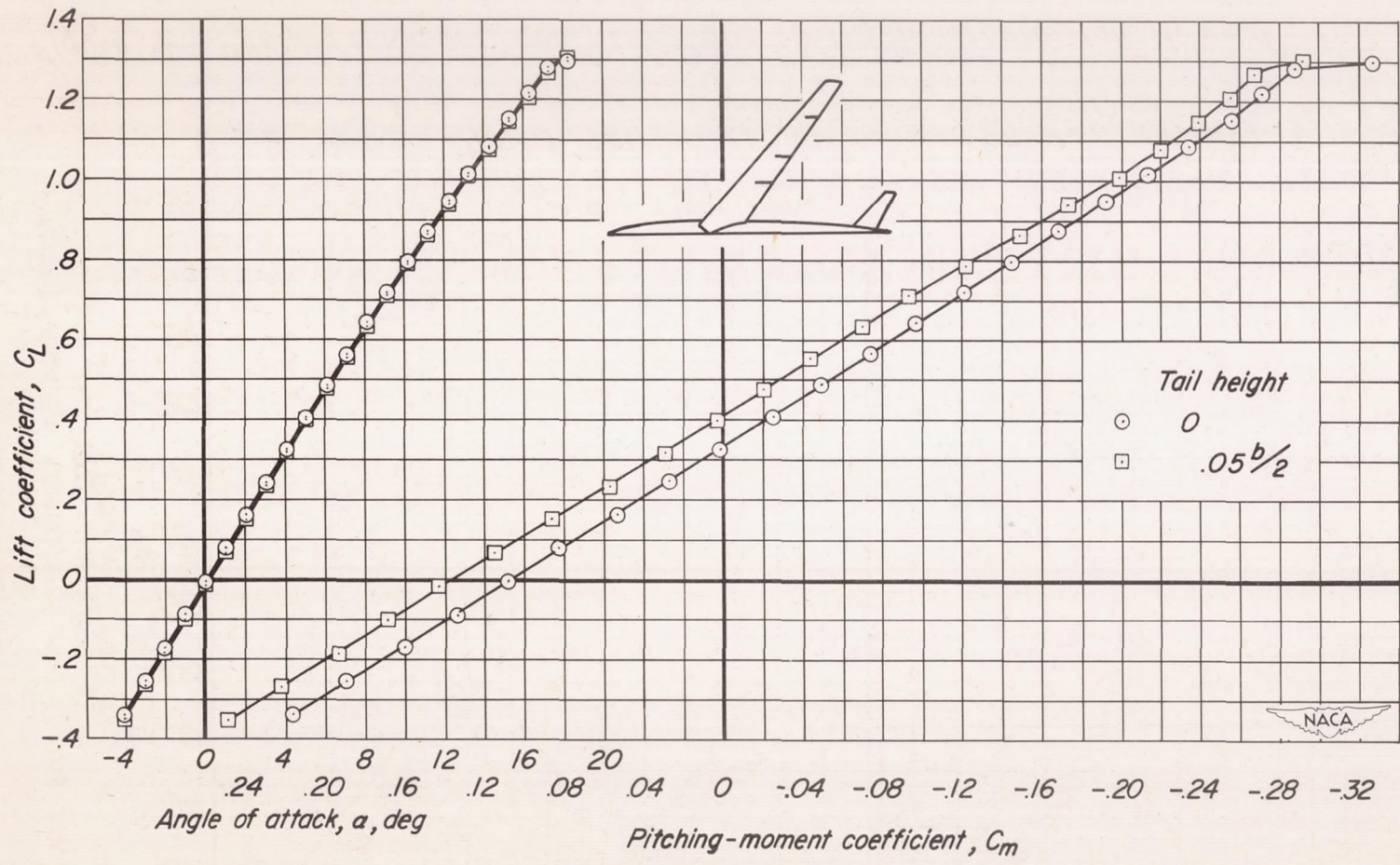


Figure 4.- Pitching-moment coefficient due to the horizontal tail. $i_t = -4^\circ$.



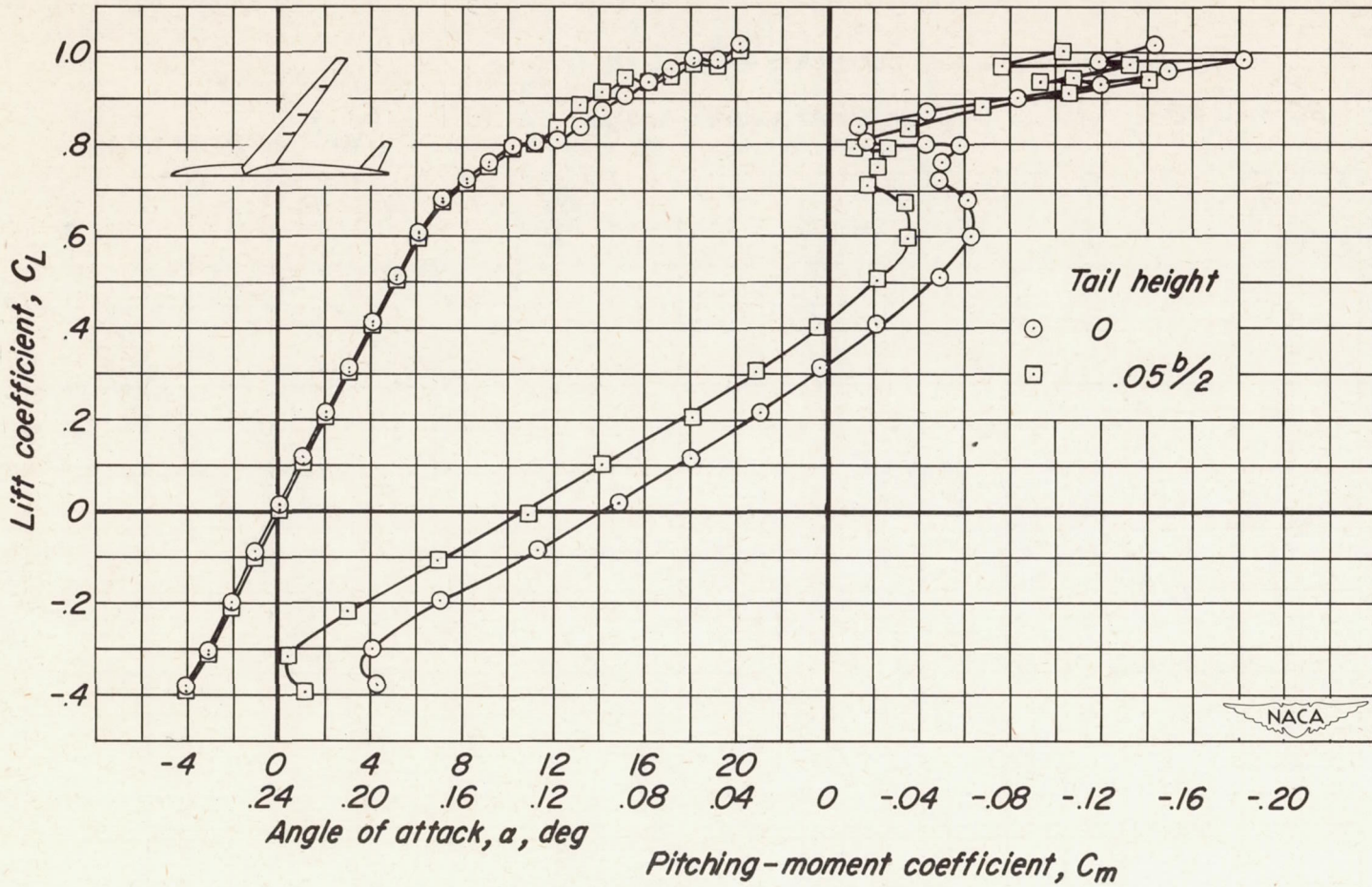
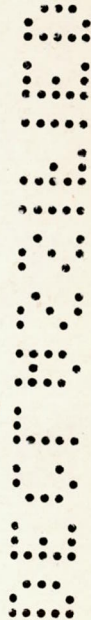


CONFIDENTIAL



(a) $M=0.25, R=8,000,000.$

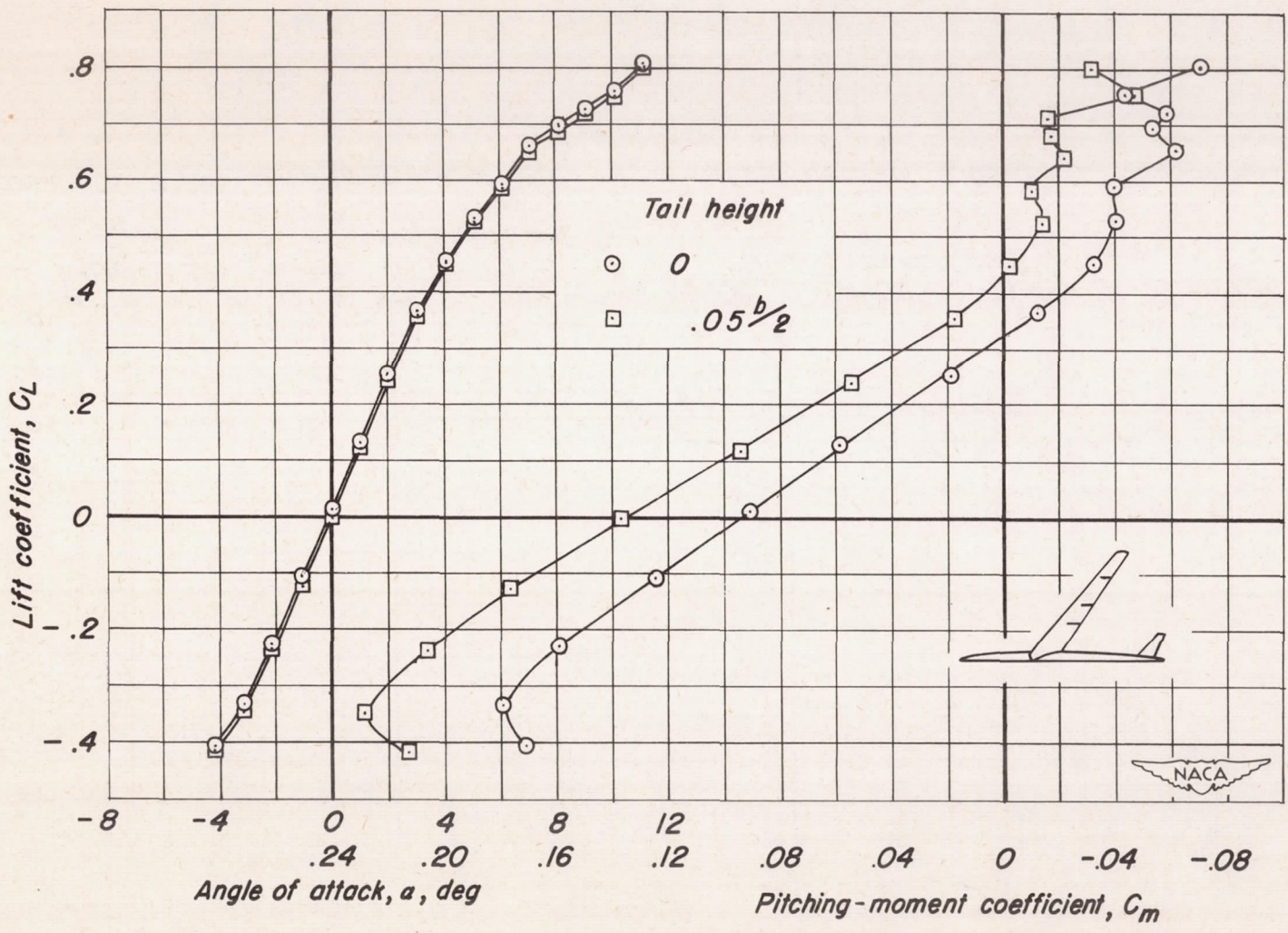
Figure 5.— The effect of a change in tail height on the lift and pitching-moment coefficients. $i_t = -4^\circ.$



(b) $M=0.80, R=2,000,000.$

Figure 5.— Continued.

CONFIDENTIAL



(c) $M=0.90, R=2,000,000.$

Figure 5.— Concluded.

CONFIDENTIAL

CONFIDENTIAL

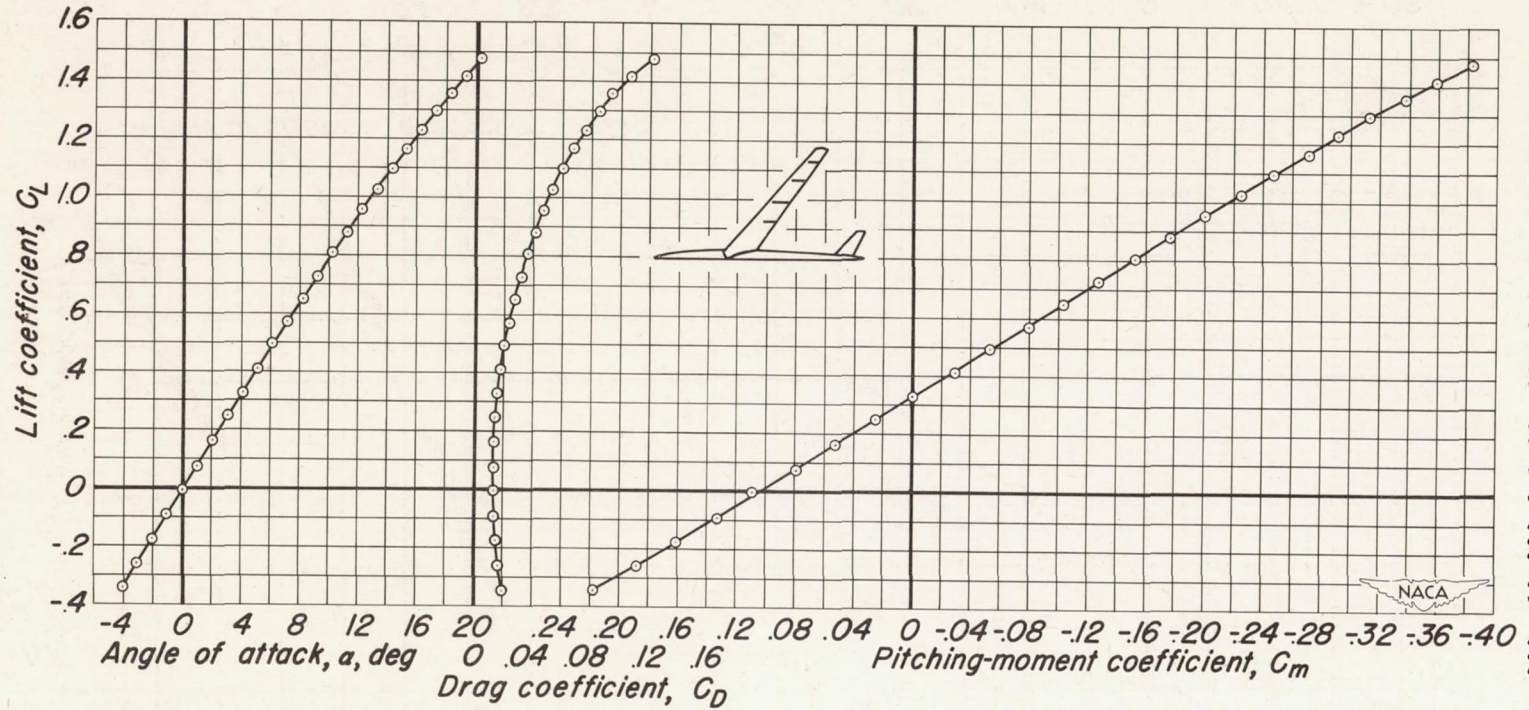
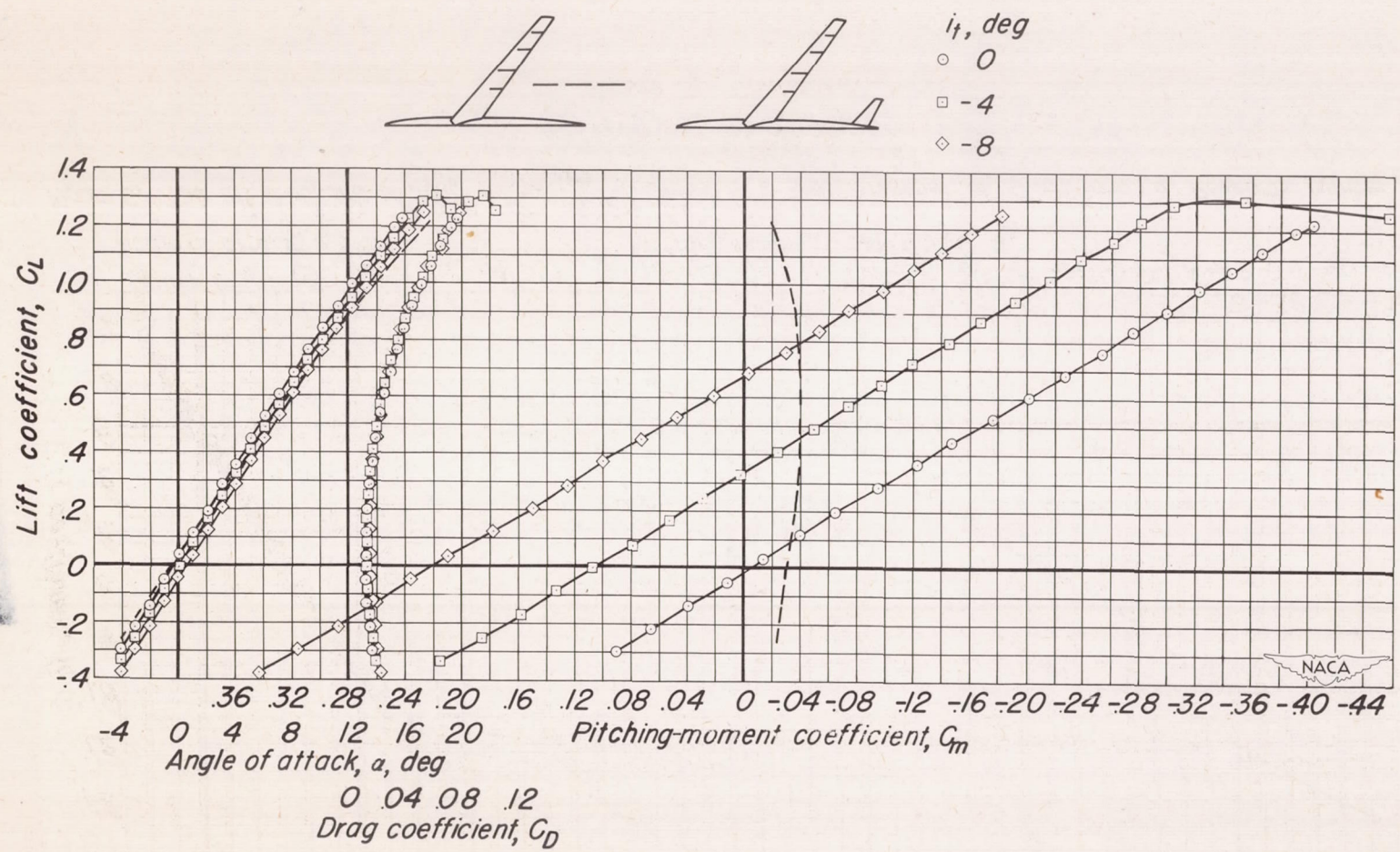


Figure 6.- The lift, drag, and pitching-moment coefficients at a Mach number of 0.165 and a Reynolds number of 8,000,000. $i_t = -4^\circ$

CONFIDENTIAL
NACA RM A52119

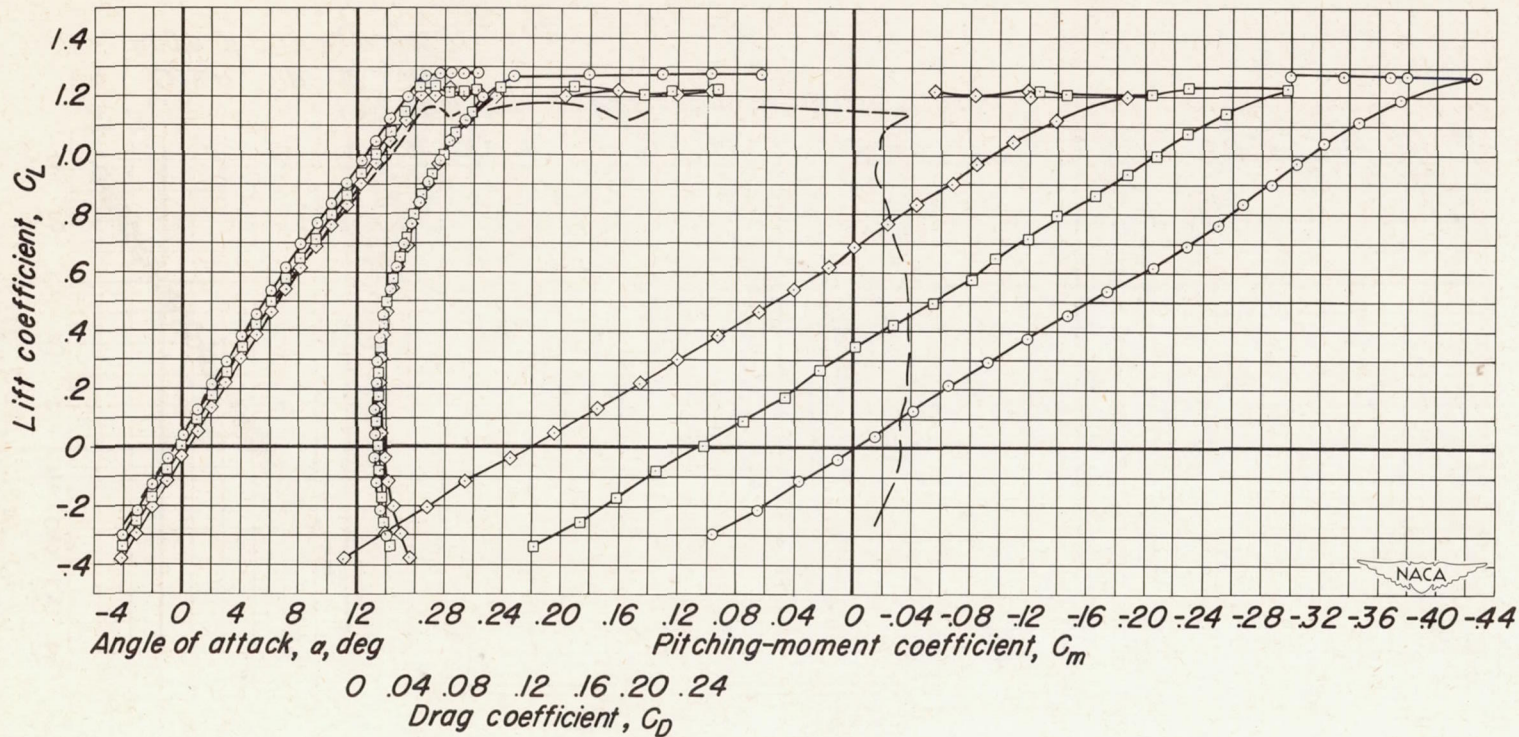
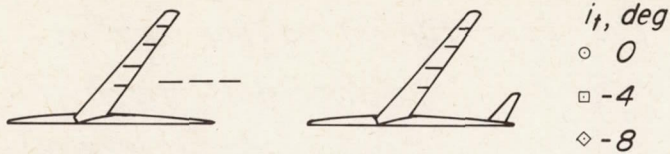
CONFIDENTIAL



(a) $M=0.25, R=8,000,00.$

Figure 7.- The effect of the horizontal tail on the lift, drag, and pitching-moment characteristics.

CONFIDENTIAL

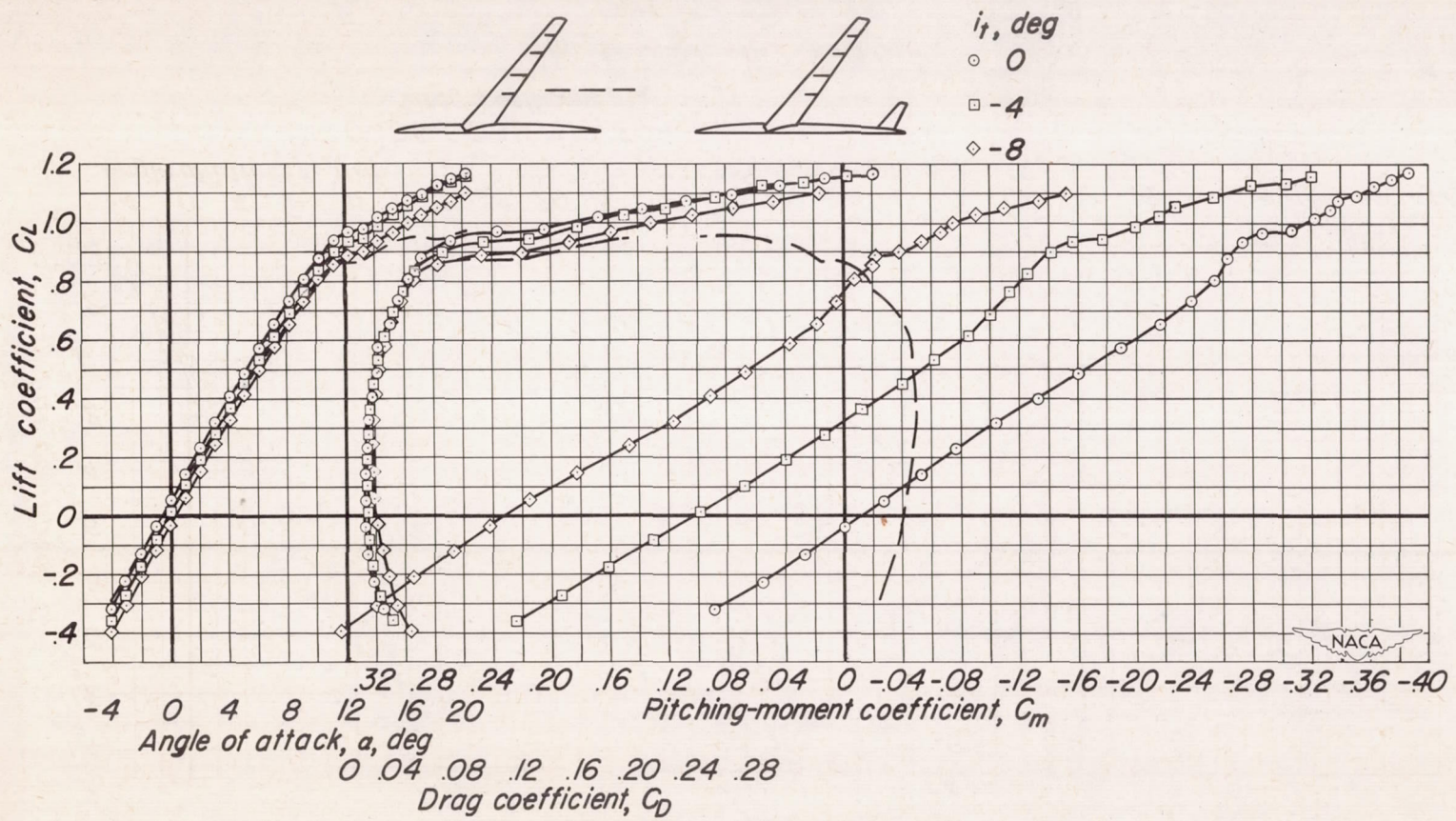


(b) $M=0.25, R=2,000,000.$
 Figure 7.- Continued.

CONFIDENTIAL

CONFIDENTIAL
 NACA RM A52119

CONFIDENTIAL

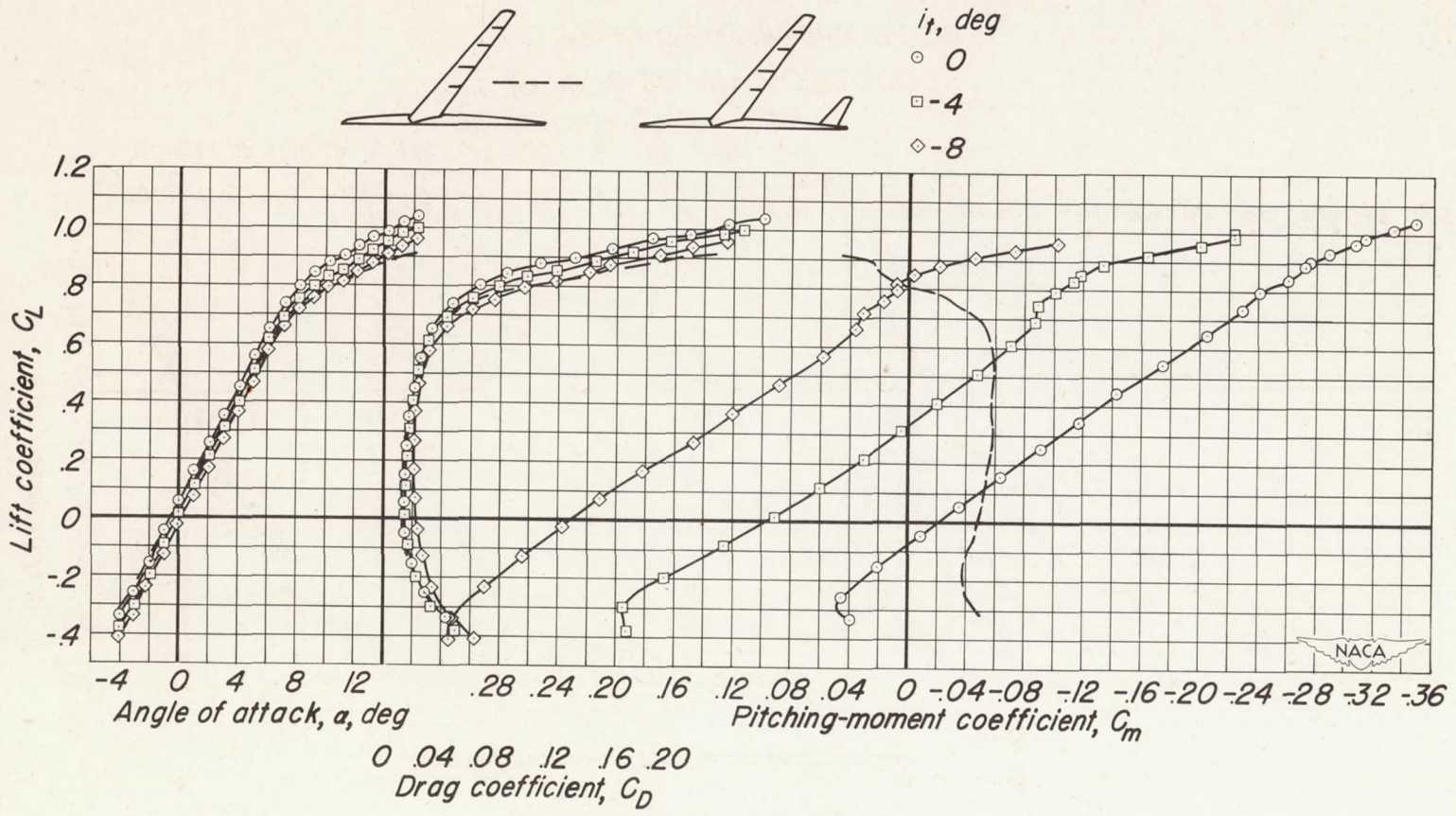


CONFIDENTIAL

(c) $M=0.60, R=2,000,000.$
 Figure 7.- Continued.

CONFIDENTIAL

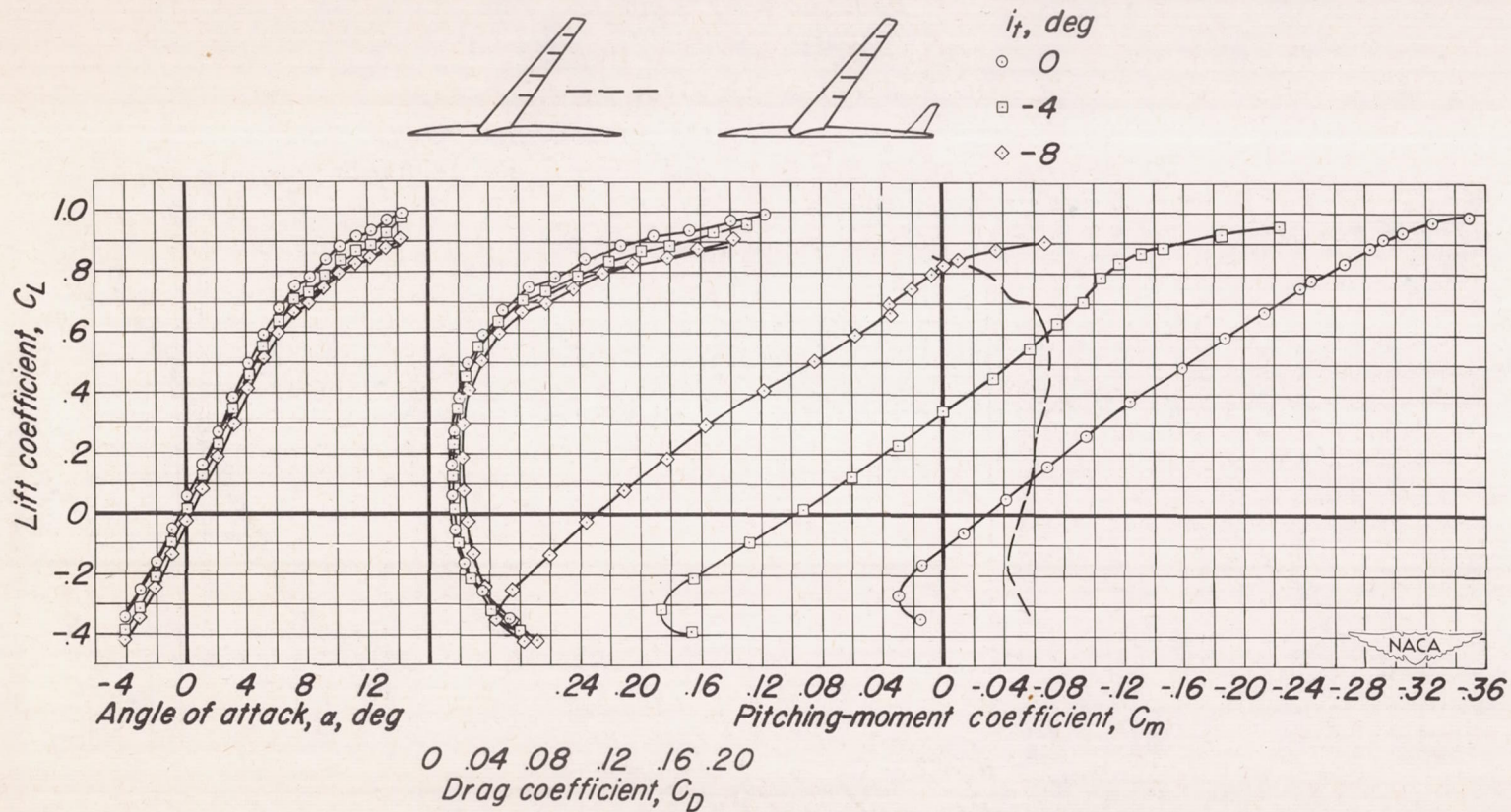
CONFIDENTIAL



(d) $M=0.80, R=2,000,000.$

Figure 7.- Continued.

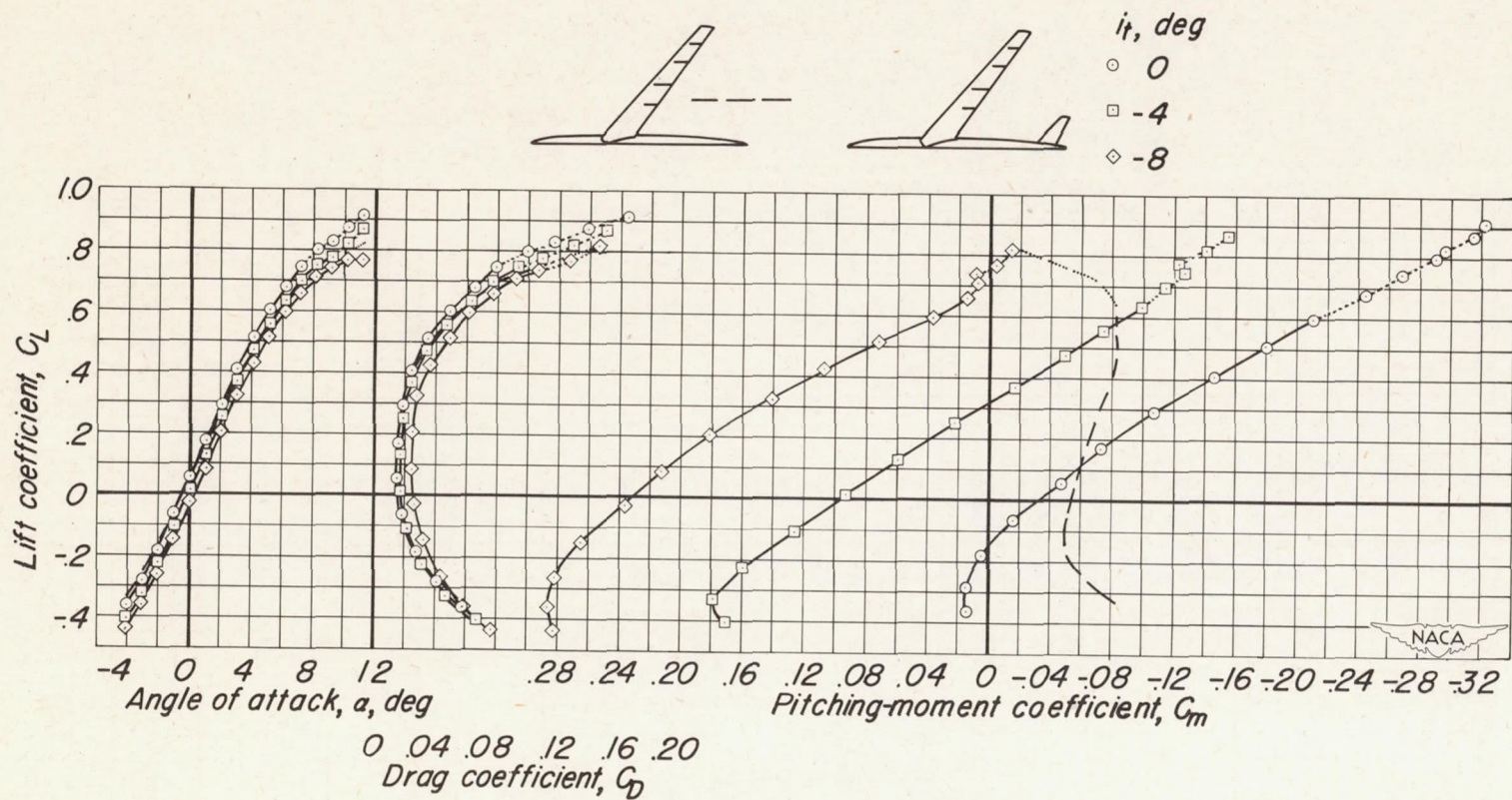
CONFIDENTIAL



(e) $M=0.86, R=2,000,000.$

Figure 7.- Continued.

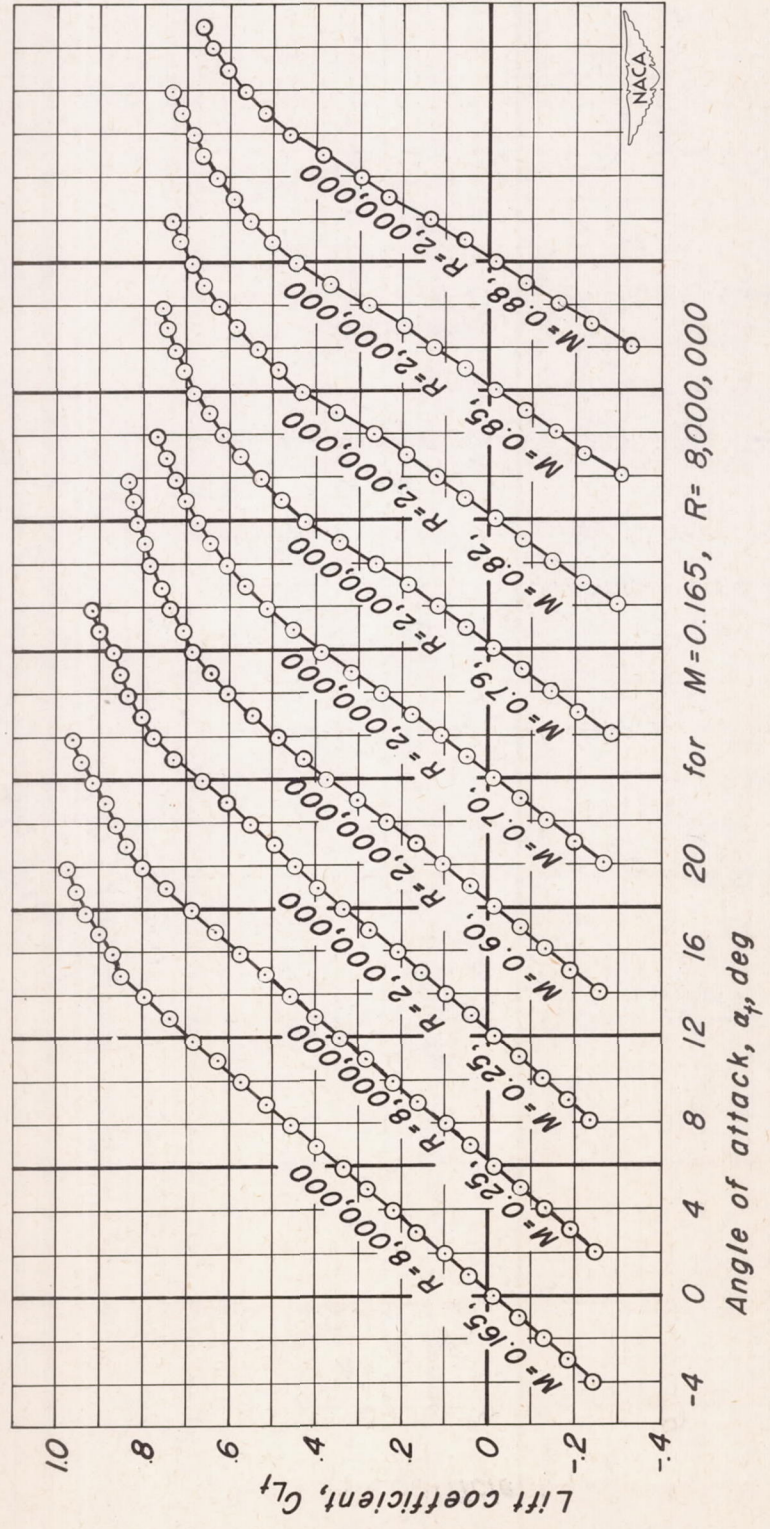
CONFIDENTIAL



(f) $M=0.90, R=2,000,000.$

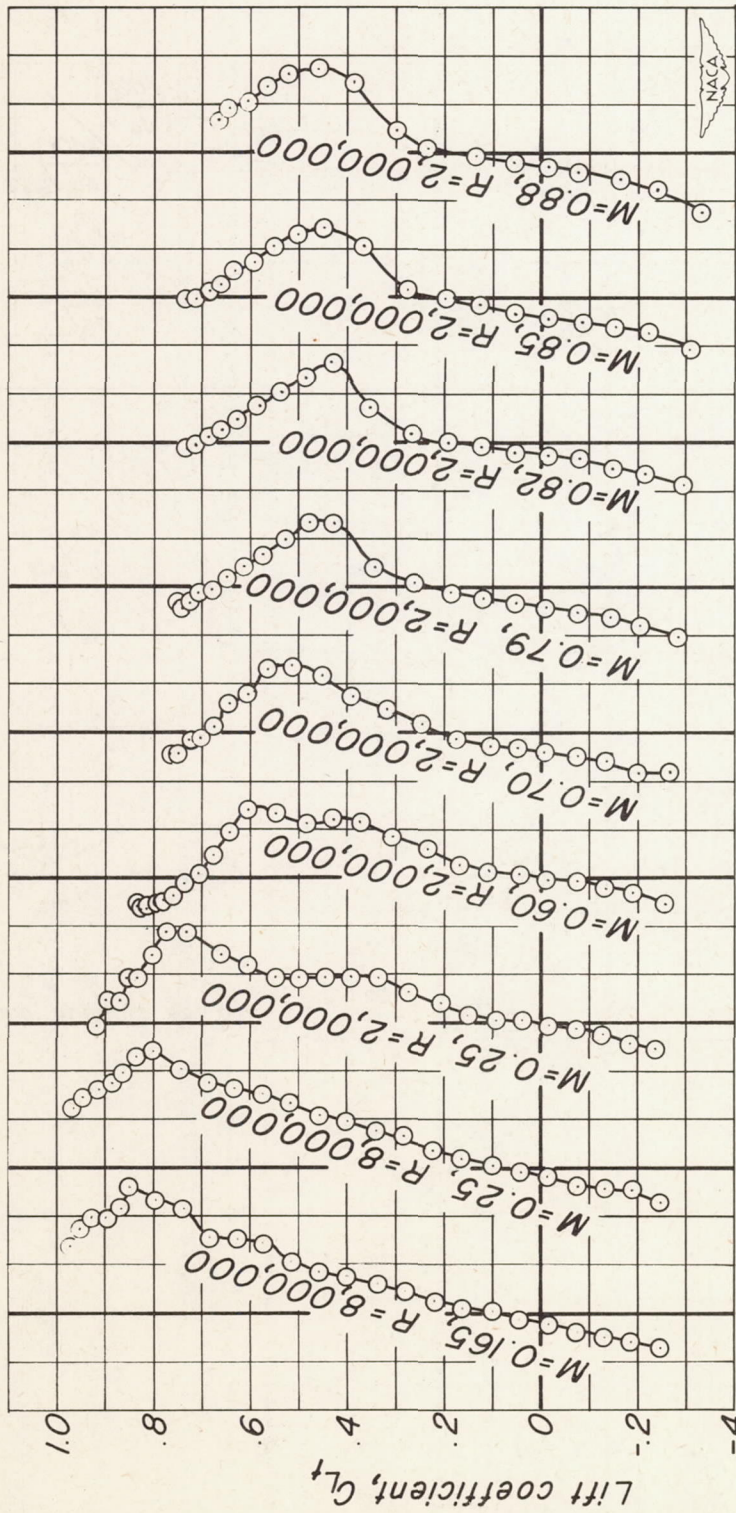
Figure 7.- Concluded.

CONFIDENTIAL



(a) C_{L_t} vs α_t .

Figure 8.— The lift and pitching-moment coefficients of the isolated horizontal tail.



Pitching-moment coefficient, C_m

(b) C_m vs C_L .

Figure 8.- Concluded.

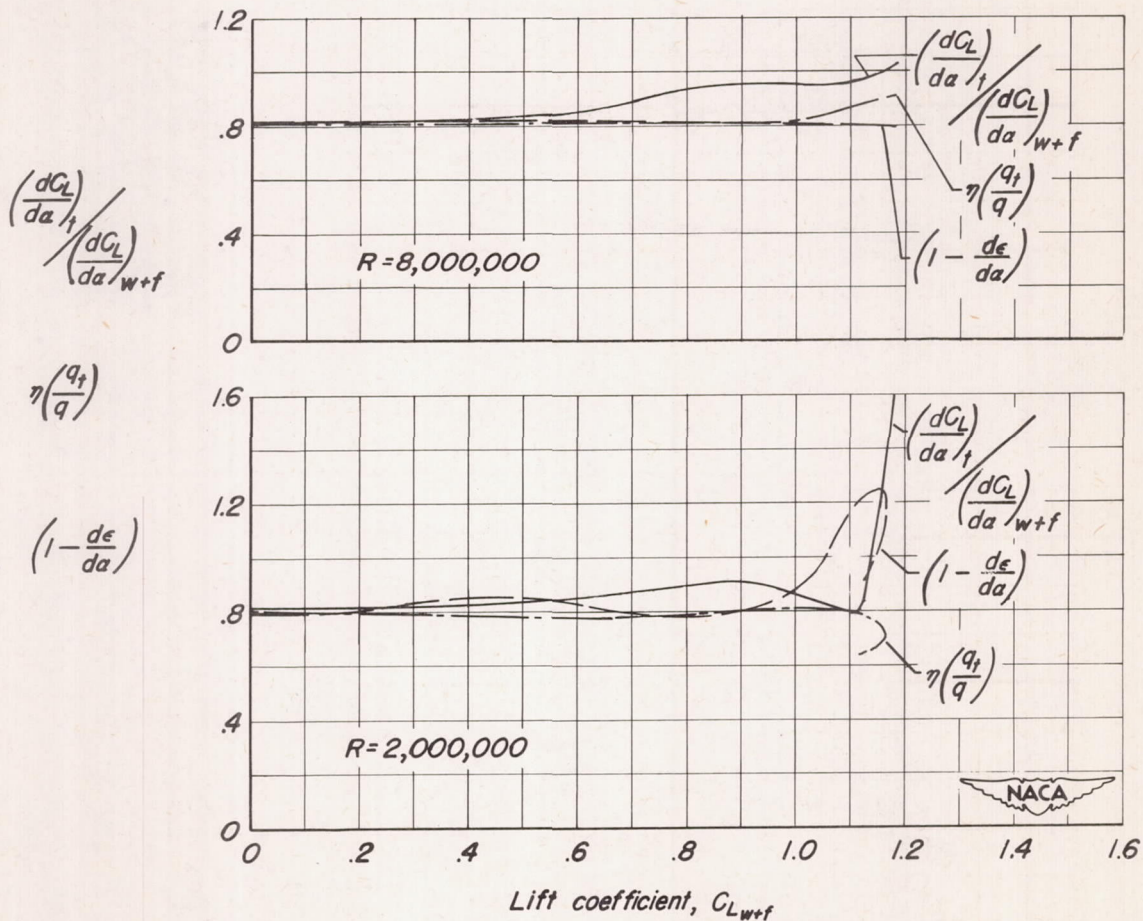


Figure 9.- The variation with lift coefficient of the factors affecting the stability contribution of the horizontal tail. $M=0.25$.

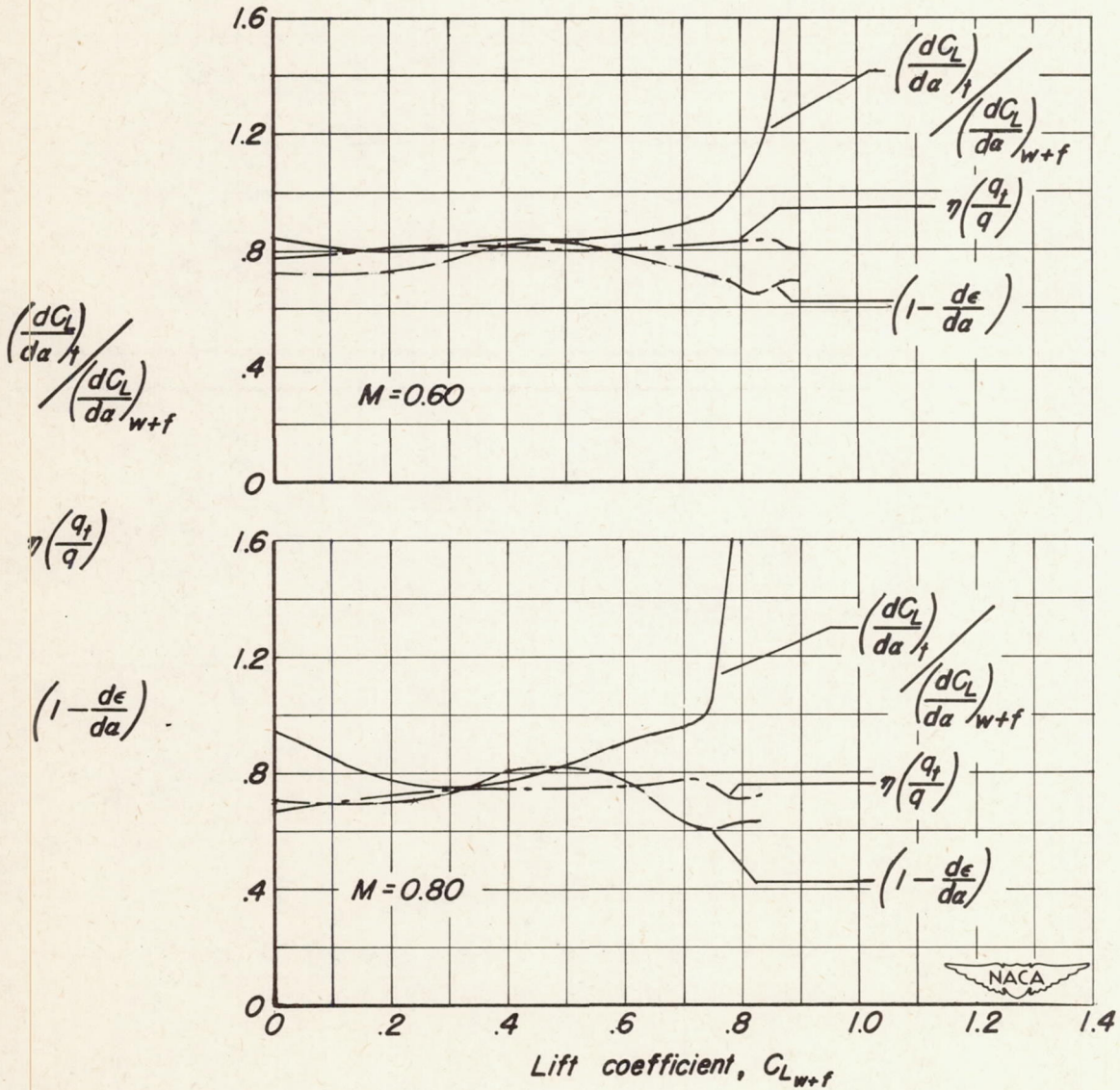


Figure 10.— The variation with lift coefficient of the factors affecting the stability contribution of the horizontal tail for two Mach numbers.

$R = 2,000,000$.

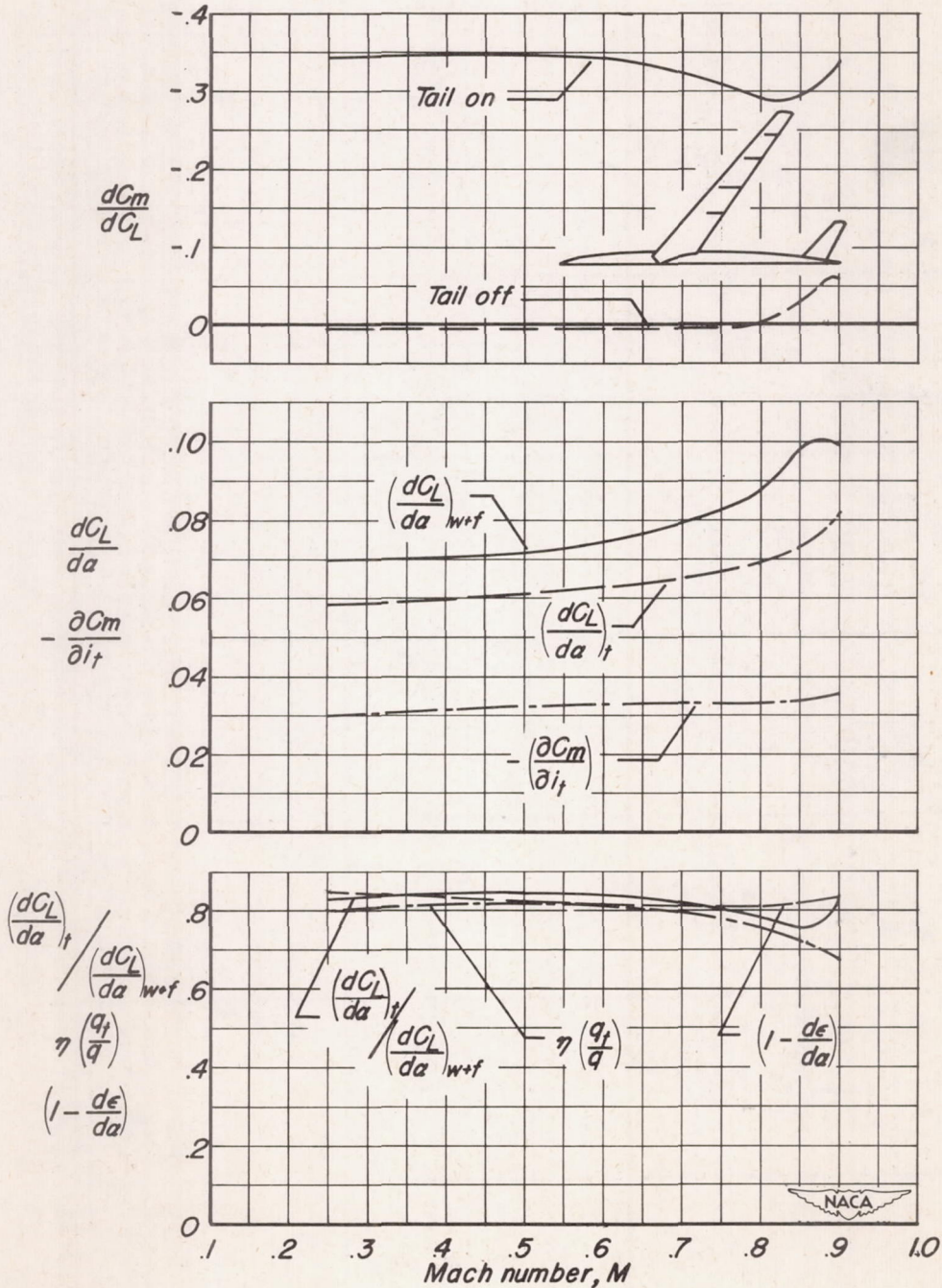
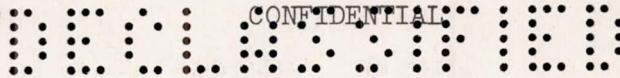


Figure 11.— The variations with Mach number of the tail control effectiveness, the static longitudinal stability, and the factors contributing to the static longitudinal stability. $C_L=0.4$, $R=2,000,000$.

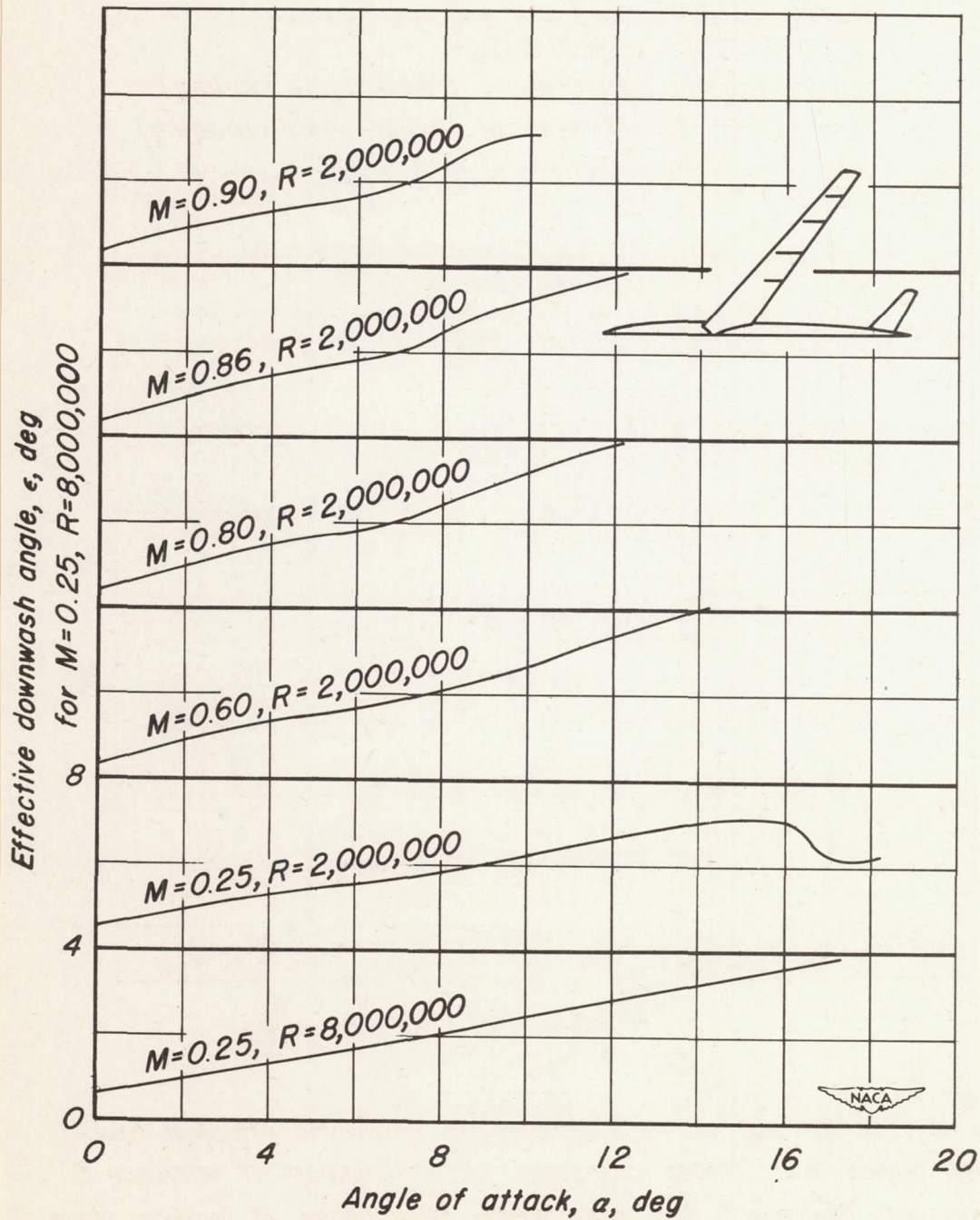


Figure 12.— The variation with angle of attack of the effective downwash angle in the plane of the root chord and leading edge as evaluated from the force data.

SECRET

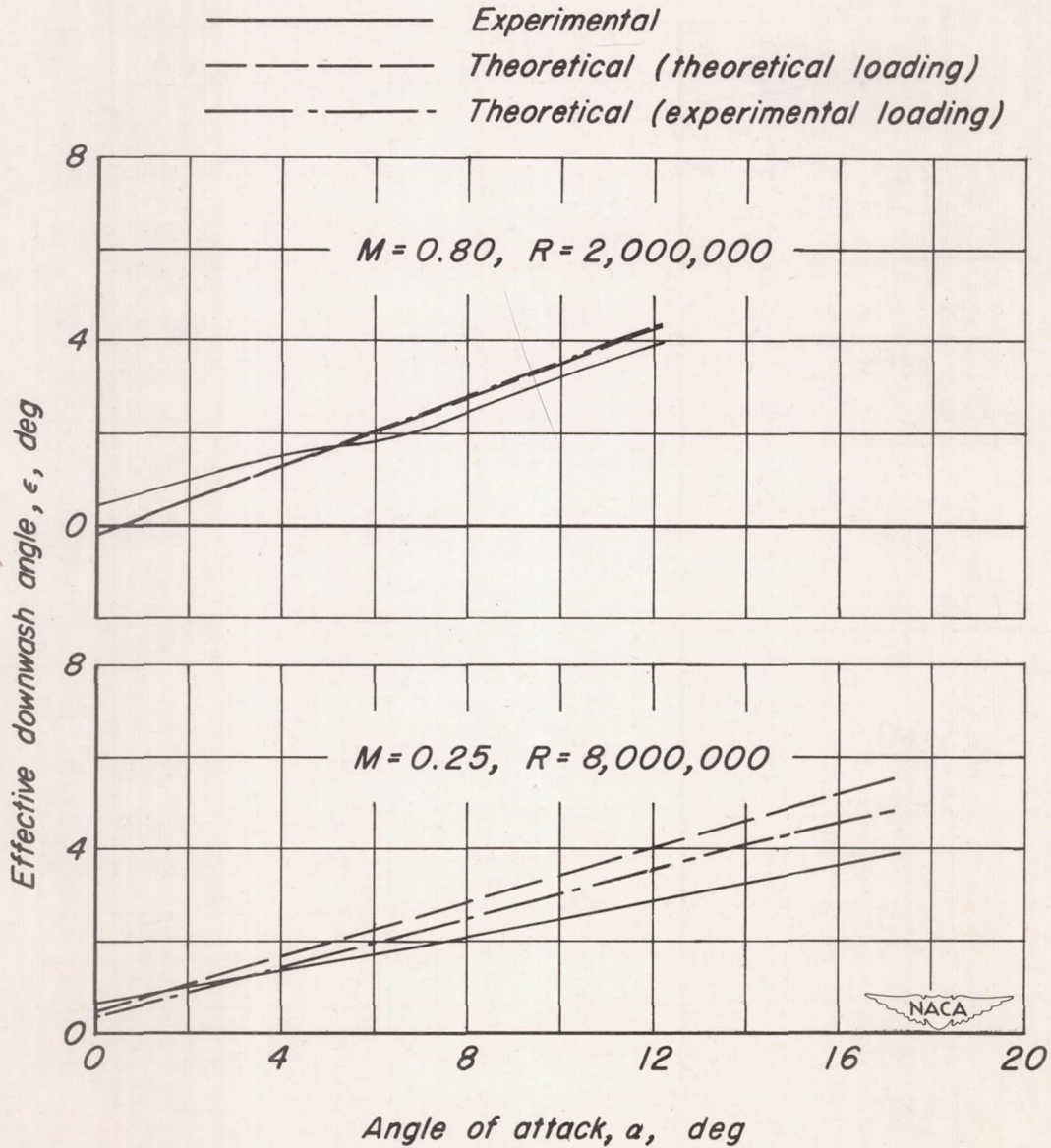


Figure 13.— Comparison of the experimentally evaluated effective downwash angles with values calculated by the method of reference 5 using both theoretical and experimental distributions of loading along the span.

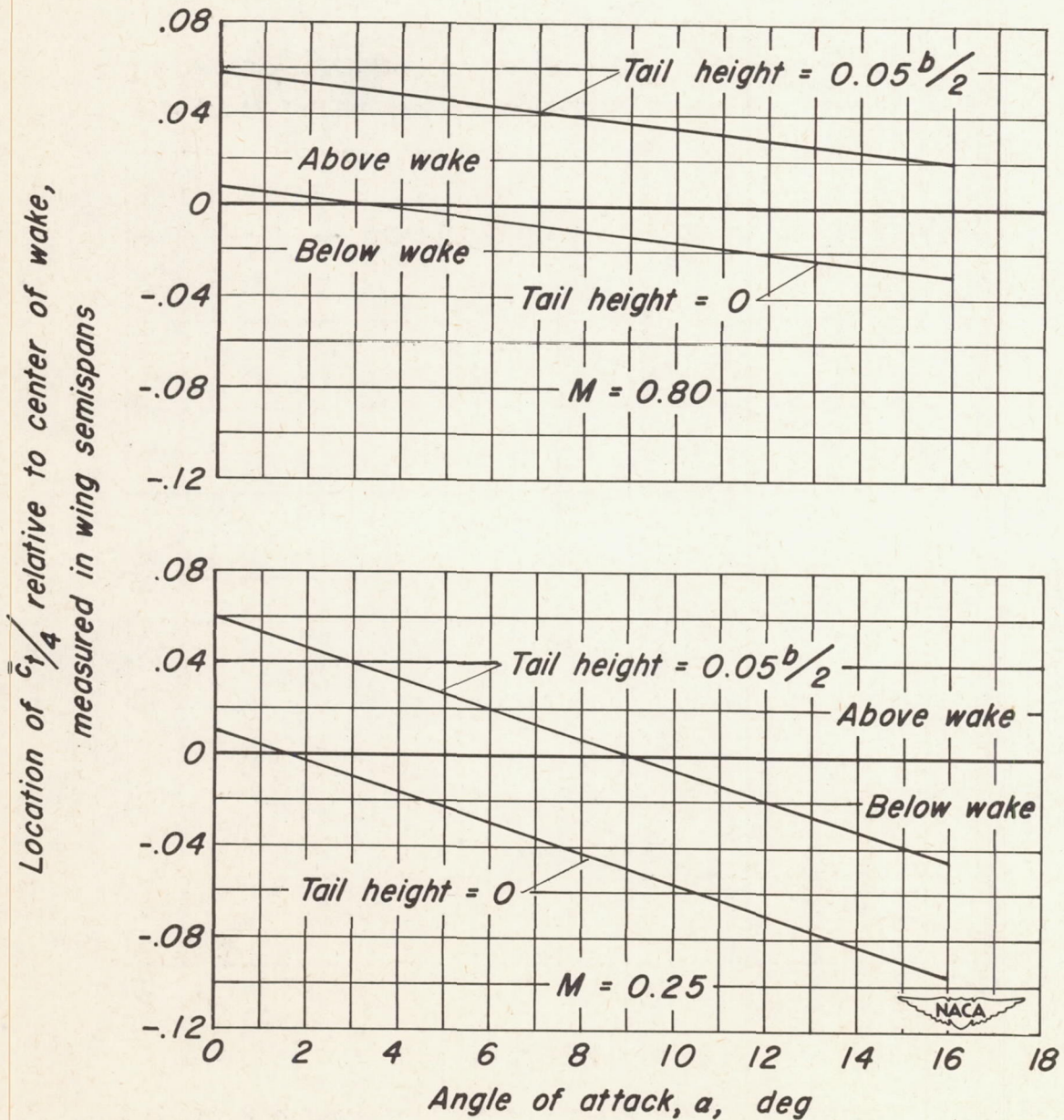


Figure 14.- The location of the horizontal tail with respect to the center of the wake as evaluated by the theoretical method of reference 5. $i_t = 0$.

CONFIDENTIAL

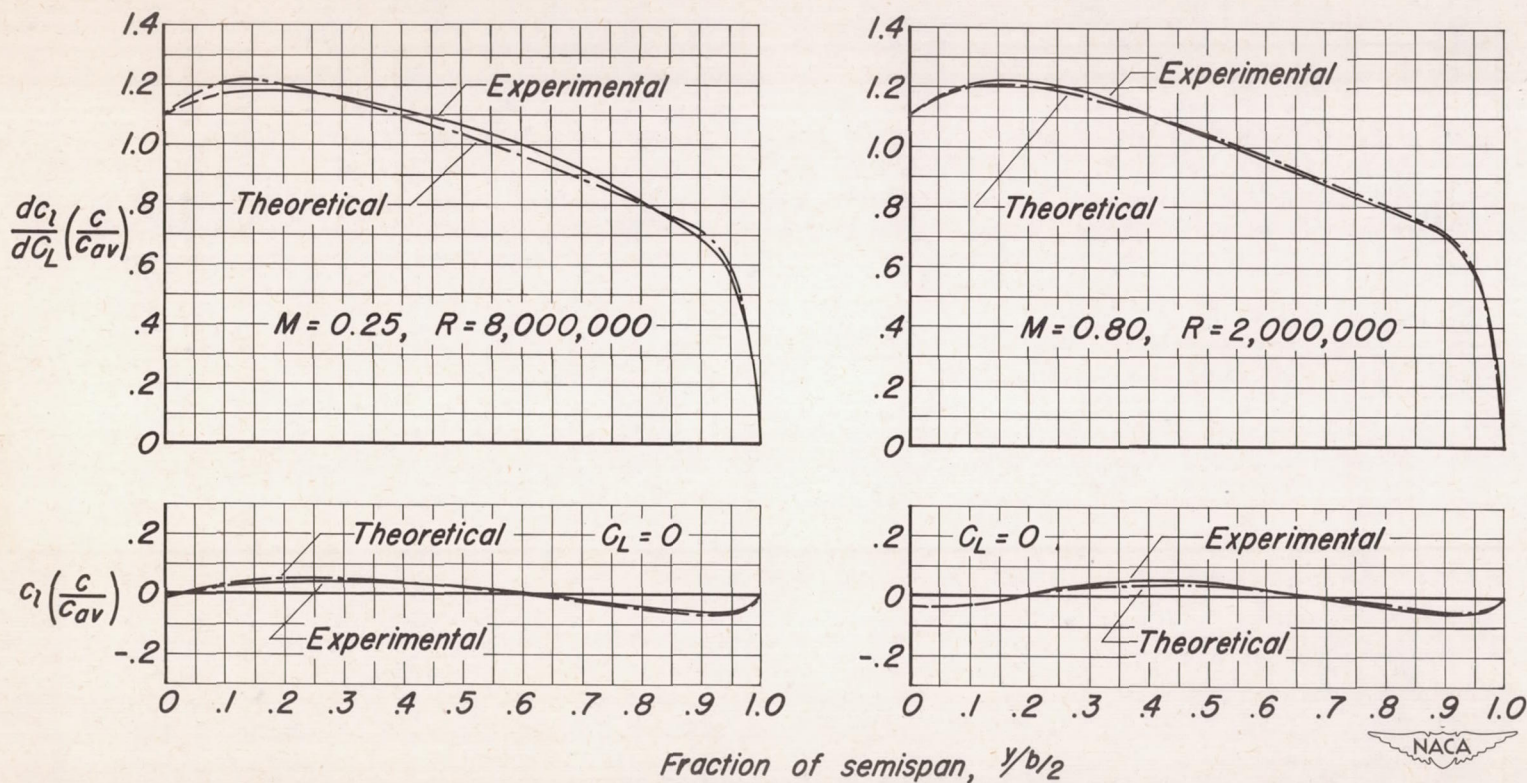


Figure 15.— The distributions of additional and basic loading along the span as calculated by the modified Falkner 19x1 method and as determined from unpublished experimental results. A549.

03712201930